

# Classification of Functional Data by Detecting the Discrepancy of Second Moment Structure of Scaled functions

Shuhao Jiao<sup>\*1</sup>, Ron D. Frostig<sup>†2</sup>, and Hernando Ombao<sup>‡1</sup>

<sup>1</sup>Statistics Program, KAUST, Saudi Arabia

<sup>2</sup>Department of Neurobiology and Behavior, UC Irvine, USA

## Abstract

This article presents a new classification method for functional data. We consider the case where different groups of functions have similar means so that it is difficult to classify them using only the mean function. To overcome this limitation, we propose the second moment-based functional classifier (SMFC). Here, we demonstrate that the new method is sensitive to divergence in the second moment structure and thus produces lower rate of misclassification compared to competitor methods. Our method uses the Hilbert-Schmidt norm to measure the divergence of second moment structure. One important innovation of our classification procedure lies in the dimension reduction step, where the SMFC method data-adaptively determines the basis functions that account for the difference

---

<sup>\*</sup>shuhao.jiao@kaust.edu.sa

<sup>†</sup>rfrostig@uci.edu

<sup>‡</sup>hernando.ombao@kaust.edu.sa

of second moment structure rather than the functional principal component of each individual group, and good performance can be achieved as unnecessary variability is removed so that the classification accuracy is improved. Consistency properties of the classification procedure and the relevant estimators are established. Simulation study and real data analysis on phoneme and rat brain activity trajectories empirically validates the superiority of the proposed method.

**Keywords:** Centroid method classifier, Cross-validation, Dimension reduction, Electroencephalogram, Functional data analysis, Second moment structure.

# 1 Introduction

Classification is a popular tool for functional data analysis. The standard problem setting is, two groups of functions with some kinds of difference are available, and we need to classify new objects with unknown group index to the correct group. The existing classification methods for functional data usually assume the two groups have different mean functions. However, functional data of different groups sometimes present similar mean functions. A common nontrivial example is electroencephalogram (EEG) recordings, where the records of each epoch always oscillate around zero. The motivation of this work comes from discriminating pre-stroke and post-stroke local field potential trajectories of rats brain. Figure 1 represents 20 sample trajectories of the first channel before and after the stroke. In such case, the classification methods based on the mean function will not be helpful. Motivated by this challenge, we propose a new classification method for functional data with similar mean functions.

The main contribution of this work is that we develop a second moment based functional classifier for the classification of different groups of functional data with similar mean function. Compared with the existing methods, we do not make any distributional

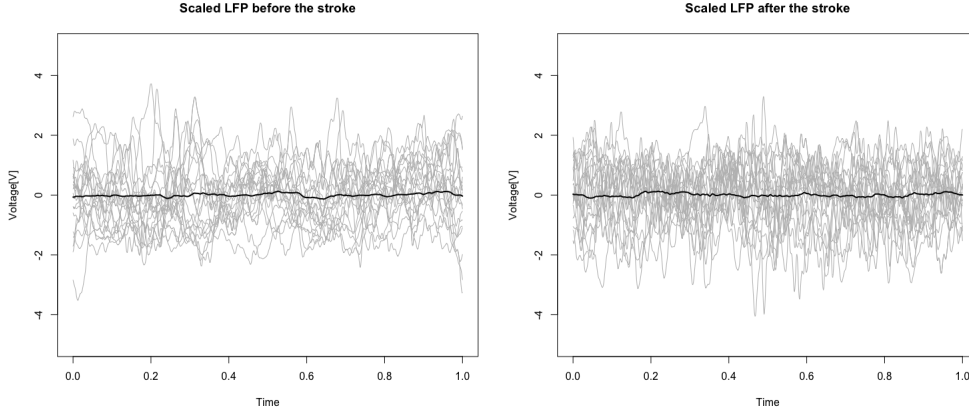


Figure 1: The first 20 pre-stroke/post-stroke functions of the first channel. Black curves are mean functions

assumption and thus the classification procedure can be widely applied. We would like to stress that, the classification accuracy is influenced by two factors, discrepancy between groups and the variability of the object to be classified. As we use more basis functions to compare different groups, the discrepancy can become more pronounced, but meanwhile, the variability will also increase. Essentially this is a trade off between bias and variance. Therefore, it is not always good to incorporate more basis functions. We propose to use the basis function that can account for the most discrepancy between groups. This is important as we can remove unnecessary variability to improve the classification accuracy. We also would like to stress that, the performance of proposed classifiers can tend to be perfect as the samples size increase. In other words, the misclassification rate can go to zero as the sample size goes to infinity. The asymptotically perfect classification can be achieved in the case that the functional trajectories present pronounced discrepancy in the second moment over a wide range of frequency and comparatively small variability. This is a similar point discussed in Delaigle & Hall (2012), and we state that this property still holds for our second-moment based functional classifier. More discussion can be found in Section 3.2.

In the past two decades, a variety of classification and clustering methods for functional data have been proposed. James & Hastie (2001) extended linear discriminate analysis

to functional data and used a parametric model to reduce the rank. Preda et al. (2007) applied partial least squares in functional linear discriminate analysis. James & Sugar (2003) developed a flexible model-based procedure. Biau et al. (2005) and Fromont & Tuleau (2006) applied nearest neighbor rule in functional data classification, and their methods are based on the first moment. Müller et al. (2005) studied generalized functional linear model, which was used for classification in Leng & Müller (2006). Li et al. (2018) used multinomial logistic model for multi-class functional data classification. Chiou & Li (2007) proposed a novel functional principal component (fPC) subspace-projected  $K$ -centers functional discrimination approach. Chiou & Li (2008) proposed a correlation-based  $K$ -centers functional clustering method. Wang et al. (2007) and Fryzlewicz & Ombao (2009) employed wavelet methods. Tian & James (2013) proposed an interpretable dimension reduction technique for functional data classification. Delaigle & Hall (2012) studied a novel functional linear classifier, which is optimal under normality and can be perfect as sample size diverges. Delaigle & Hall (2013) also studied the functional Bayesian quadratic classifier and applied it to censored functional data. Ieva et al. (2016) proposed a new algorithm to perform clustering of functional data based on covariance, where the true group index is assumed unknown. Wang et al. (2016) gave an overall overview of the existing classification method for functional data. Most of these works highly depend on the discrepancy between first moments, which motivates us to develop a classification methodology for groups with similar means. Some of these methods also incorporate the covariance difference, (e.g. Chiou & Li (2007) and Delaigle & Hall (2013)), however, in the methods, the discrepancy between second moments is accounted for by group-wise fPCs, which can not capture the discrepancy efficiently. Pigoli et al. (2014) discussed different distances for covariance operators.

Meanwhile, there are some research works on discriminating multivariate data by covariance. Anderson et al. (1962) and Hoffbeck & Landgrebe (1996) studied classification procedures for observations coming from one of two multivariate normal distributions in

the case that the two distributions differ both in mean vectors and covariance matrices. Madiraju & Liu (1994) proposed a simple and powerful approach for texture classification using the eigen-features of local covariance measures. Kluckner & Bischof (2009), Fehr et al. (2012) and Fehr et al. (2014) used covariance descriptor in the classification of multivariate data. In EEG-based classification, Farquhar (2009) and Barachant et al. (2013)) used spatial covariance matrix as a feature. Sundararajan et al. (2019) proposed a FS-ratio statistics and used it as a feature to discriminate different states. Fontaine et al. (2019) proposed a copula-based algorithm to detect changes in brain signals. These methods use different features to discriminate epochs under different states. However, since the intra-curve information is not incorporated, the methods will not perform well if the discrepancy is mainly present in the intra-curve structure.

Compared with the existing methods, our method has the following advantages:

- The proposed classification procedure is entirely data-driven and non-parametric, making it a suitable method for a broad range of data.
- We use the sequence of orthonormal basis, that account for most of the discrepancy of the second moments, in comparison to improve the classification accuracy.
- Our method takes account of the intra-curve information, which is important in functional trajectories.
- We extend the procedure to correlated and multivariate functional data.

The rest of the paper is organized as follows. In Section 2, we introduce some preliminaries of functional data. In Section 3, we present the classification procedure in the cases of independent, multivariate and correlated functional data, and shows the consistency of the classification procedure and the relevant estimators. In Section 4, we study the finite sample properties of the procedure by simulations, and compare our method with some competitor methods. In Section 5, we implement the proposed

method to classify different phonemes and different states of rats brain activity. Conclusion is made in Section 6. Technical proofs, some relevant algorithms and additional figures can be found in the appendix.

## 2 Preliminaries

- The notation  $X \in L^p(H)$  indicates that, for some  $p > 0$ ,  $\int_H |X(t)|^p dt < \infty$ . Let  $(X_k(t): k \in \mathbb{N})$  be a set of functional trajectories such that each function is an element of the Hilbert space  $L^2([0, 1])$ , where the inner product is defined as  $\langle x, y \rangle = \int_0^1 x(t)y(t)dt$ , and the norm is defined as  $\|x\|^2 = \int_0^1 x(t)^2 dt$ .
- Assume  $E(\int X^2(t)dt) < \infty$ , we define the mean function by

$$\mu(t) = E[X(t)],$$

and the second moment operator  $C: L^2[0, 1] \rightarrow L^2[0, 1]$  by

$$C(x) = \mathbb{E}[\langle X, x \rangle X].$$

- By Mercer's theorem, we have the following expression of the symmetric positive-definite compact operator  $C(x)$ ,

$$C(x) = \sum_{j=1}^{\infty} \lambda_j \langle v_j, x \rangle v_j,$$

where  $(\lambda_j: j \in \mathbb{N}_+)$  are the positive eigenvalues (in strictly descending order) and  $(v_j: j \in \mathbb{N}_+)$  are the corresponding normalized eigenfunctions, so that  $C(v_j) = \lambda_j v_j$  and  $\|v_j\| = 1$ .

- The Hilbert–Schmidt norm of a Hilbert-Schmidt operator  $\Phi$  is defined as:

$$\|\Phi\|_{\mathcal{S}}^2 = \sum_{i,j} |\Phi_{i,j}|^2,$$

where  $\Phi_{i,j} = \langle \Phi(e_i), e_j \rangle$ , and  $\|\Phi\|_{\mathcal{S}} < \infty$ .  $(e_i: i \in \mathbb{N}_+)$  is a sequence of orthonormal basis functions. This norm does not depend on the choice of  $(e_i: i \in \mathbb{N}_+)$ .

### 3 Model, consistency, and algorithm

#### 3.1 General setting

Suppose we have a sequence of functions in  $L^2([0, 1])$  for each group,

$$X_1^{(g)}(t), X_2^{(g)}(t), \dots, X_{n_g}^{(g)}(t), \quad g = 0, 1, \text{ and } n_0 + n_1 = N,$$

where  $g$  is the group index. We define group mean function and second moment function at lag  $h$  of the scaled functions as

$$\begin{aligned} E[X_k^{(g)}(t)] &= \mu_g(t), \\ C_g^{(h)}(x) &= \int E \left( \frac{X_k^{(g)}(t) X_{k+h}^{(g)}(s)}{\|X_k^{(g)}(t)\| \|X_{k+h}^{(g)}(s)\|} \right) x(s) ds, \\ C_g^{(-h)}(x) &= \int E \left( \frac{X_{k+h}^{(g)}(t) X_k^{(g)}(s)}{\|X_{k+h}^{(g)}(t)\| \|X_k^{(g)}(s)\|} \right) x(s) ds, \end{aligned}$$

where  $h = 0, 1, 2, \dots$ . In practice,  $(c_g^{(h)}(t, s): h \in \mathbb{N}, \dots, g = 0, 1)$  are unknown, and we can estimate them by the following empirical estimator

$$\hat{C}_g^{(h)}(x) = \int \frac{1}{n_g - h} \sum_{k=1}^{n_g - h} (X_k^{(g)}(t) / \|X_k^{(g)}\|) (X_{k+h}^{(g)}(s) / \|X_{k+h}^{(g)}\|) x(s) ds,$$

$$\hat{C}_g^{(-h)}(x) = \int \frac{1}{n_g - h} \sum_{k=1}^{n_g - h} (X_{k+h}^{(g)}(t) / \|X_{k+h}^{(g)}\|) (X_k^{(g)}(s) / \|X_k^{(g)}\|) x(s) ds.$$

Here we assume that  $\mu_1 - \mu_2$  is close to zero, so that it is very hard to classify two groups by mean function difference, then we need to check the second moment structure of two groups. An important step is scaling. Without it, objects in the group with higher variability would be more likely to be misclassified into the group with lower variability. The scaling step prevents the magnitude of variability to interfere with detection of the difference of second moment structure. In the following of the article, we assume all functions are already scaled to norm one. If the variability of two groups are significantly different, say, the variability of one group is significantly greater than the other one, we can set a threshold for the norm of the functions, and pre-classify the functional objects by thresholding. More specifically, if the norm of a function exceeds the threshold, then we can classify it into the group with higher variability.

**Remark:** We compare second moment functions instead of covariance functions, as second moment function incorporates mean function. If the mean functions of the two groups are slightly different, that discrepancy will contribute to the group discrimination.

## 3.2 Independent functions

We assume  $(X_k^{(g)}(t) : k \in \mathbb{N}_+)$  are independent functions, and suppose  $Y$  is a new object to be classified. Our centroid classifier assigns  $X$  to  $\Pi_g$  if

$$D(Y \langle Y, x \rangle, C_g^{(0)}(x)) < D(Y \langle Y, x \rangle, C_{1-g}^{(0)}(x)),$$



where  $D$  is a metric distance of Hilbert-Schmidt operator. The distance we use in this article is induced by Hilbert-Schmidt norm, which is given by

$$D(Y\langle Y, x \rangle, C_g^{(0)}(x)) = \sum_{i,j}^{\infty} \langle (Y\langle Y, \nu_i \rangle - C_g^{(0)}(\nu_i)), \nu_j \rangle^2,$$

where  $(\nu_i: i \in \mathbb{N}_+)$  are orthonormal basis functions.

**Remark:** The log-Euclidean metric and the affine invariant Riemannian metric are popular for finite-dimensional covariance matrix. However, the matrix logarithm is not extended to infinite-dimensional trace-class functional operators. The eigenvalue  $\lambda_i$  of second moment operator typically converge to zero, making it difficult to extend those distance to functional case. Comparatively, the distance induced by Hilbert-Schmidt norm is well defined for second moment functional operators and can also produce reasonable between-group comparison. This point is also discussed in Pigoli et al. (2014).

In practice, the sample size is limited, so we need to do dimension reduction to extract the most important features that discriminate the two groups, otherwise, the bases which cannot well discriminate the two groups will reduce the classification accuracy. In other words, we propose the truncated distance for comparison, defined as

$$D_d(Y\langle Y, x \rangle, C_g^{(0)}(x)) = \sum_{i,j}^d \langle (Y\langle Y, \nu_i \rangle - C_g^{(0)}(\nu_i)), \nu_j \rangle^2.$$

If  $d$  is specified, we will omit subscript  $d$  in the notation. We aim to find a series of orthonormal basis  $(\nu_i: i = 1, \dots, d)$ , such that the difference between groups is maximized. We propose to use the eigenfunctions of the compact symmetric operator  $C(x) = (C_0^{(0)} - C_1^{(0)})^2(x)$ , where  $(C_0^{(0)} - C_1^{(0)})^2(x) = (C_0^{(0)} - C_1^{(0)})((C_0^{(0)} - C_1^{(0)})(x))$ . In Theorem 1, we have shown that, the misclassification probability is partially determined by  $\|C_0^{(0)} - C_1^{(0)}\|_S$  evaluated in a  $d$ -dimensional space, and a larger value of this norm

can result in a smaller misclassification probability. Since  $C$  is a compact symmetric positive-definite operator, and allows the spectral decomposition

$$C(t, s) = \sum_{i=1}^{\infty} \lambda_i^C \nu_i(t) \nu_i(s),$$

and by nature of Hilbert-Schmidt norm,

$$\|C_0^{(0)} - C_1^{(0)}\|_S = \sum_{i=1}^{\infty} \lambda_i^C.$$

It is noted that  $C_0^{(0)} - C_1^{(0)}$  has the same eigenfunction of  $(C_0^{(0)} - C_1^{(0)})^2$ , and the Hilbert-Schmidt norm of  $C_0^{(0)} - C_1^{(0)}$  is equal to the summation of eigenvalues of  $(C_0^{(0)} - C_1^{(0)})^2$ .  $(C_0^{(0)} - C_1^{(0)})^2$  is positive definite, so we propose to use the eigenfunctions associated with largest eigenvalues  $\lambda_i^C$  for the computation of  $\|C_0^{(0)} - C_1^{(0)}\|_S$ . In practice, the estimator of  $(C_0^{(0)} - C_1^{(0)})^2$  is  $(\hat{C}_0^{(0)} - \hat{C}_1^{(0)})^2$ .

The classification algorithm proceeds as follows:

---

**Algorithm 1** Classification algorithm for independent functions

---

- Step 1.** Fix  $d$ , obtain the eigenfunctions  $\{\hat{\nu}_j\}_{j=1}^d$  of the operator  $(\hat{C}_0^{(0)} - \hat{C}_1^{(0)})^2(x)$ .  
**Step 2.** Then compute the scores  $\hat{S}_{ij}^g = \langle \hat{c}_g^{(0)}(\hat{\nu}_i), \hat{\nu}_j \rangle$  for  $i, j = 1, \dots, d$ .  
**Step 3.** Compute difference between the scores  $\hat{S}_{ij}^g$  and the score of kernel  $Y(t)Y(s)$ , and obtain the summation of the difference over  $i, j = 1, \dots, d$ , that is,

$$\hat{D}_g = \sum_{i,j}^d (\hat{S}_{ij}^g - \langle Y, \hat{\nu}_i \rangle \langle Y, \hat{\nu}_j \rangle)^2.$$

If  $\hat{D}_0 - \hat{D}_1 < 0$ , classify  $Y$  to  $\Pi_0$ , otherwise, classify it to  $\Pi_1$ .

---

**Remark:** It is not always good to incorporate more dimensions, as more dimensions bring more variability. We introduce two methods to select  $d$ : 1). We choose the dimension  $d$ , such that the approximation accuracy of  $(C_0^{(0)} - C_1^{(0)})^2(x)$  by its first  $d$  eigenfunctions, which can be measured by  $\sum_{i=1}^d \lambda_i^C / \sum_{i>1} \lambda_i^C$ , exceeds a threshold.

2) We can apply cross validation. To be more specific, we try different values of  $d$  to do classification in the training set, and choose the  $d$  with the lowest classification rate. The same procedure can also be applied to the other two cases, say, multivariate functional data and correlated functional data, which will be discussed later.

Theorem 1 tells us the classification can be near perfect as the discrepancy between groups are large enough or sample size diverges. In the theorem, we give an upper bound of the misclassification rate. More specifically, by applying Chebyshev and Cauchy-Schwarz inequality, we find that the upper bound can be expressed as a ratio of score variability to the second moment discrepancy.

**Theorem 1.** Assume  $\|C_0^{(0)} - C_1^{(0)}\|_S > 0$  and  $E\|Y^4\| < \infty$ , the misclassification probability  $P(\Pi_{1-g}|\Pi_g)$  satisfies

$$P(\Pi_{1-g}|\Pi_g) \leq \frac{4 \sum_{i,j=1}^d \sigma_{ij}^{(g)}}{\sum_{i,j=1}^d \langle (C_0^{(0)} - C_1^{(0)}) \nu_i, \nu_j \rangle^2},$$

where  $\sigma_{ij}^{(g)} = \text{var}(\langle Y, \nu_i \rangle \langle Y, \nu_j \rangle)$ .

In practice, as the sample size  $N$  increases, we can incorporate a larger dimension  $d_N$ , and the term  $\sum_{i,j=1}^{d_N} \langle (C_1^{(0)} - C_1^{(0)}) \nu_i, \nu_j \rangle^2$  can increase with the sample size. If the variance  $\sum_{i,j=1}^{d_N} \sigma_{ij}^{(g)}$  does not increase very fast with  $N$ , the misclassification rate will converge to zero. Consider EEG recordings, assume the trajectories admit the following Fourier expansion,

$$X_k^{(g)}(t) = \sum_{j=1}^L \left( a_{kj}^{(g)} \cos(jt) + b_{kj}^{(g)} \sin(jt) \right),$$

where  $L$  is the length of each epoch. If the number of epochs increase, we can incorporate more basis functions  $(\nu_j: j = 1, \dots, d_N)$  to discriminate  $(a_j^{(0)}, b_j^{(0)})$  and  $(a_j^{(1)}, b_j^{(1)})$  over a wider range of frequency  $j$ , as  $\nu_j$  typically depicts higher frequency component as  $j$  increases. If the data of different groups presents discrepancy over a wide range of

frequency band, the classification can be near perfect as the sample sizes go to infinity.

### 3.3 Multivariate functional data

Assume we simultaneously observe  $M$  functions  $X_{km}^{(g)}(t)$ ,  $m = 1, \dots, M$ , for each  $k$ , and the second moment structure of two groups are different for each set, we aim to jointly classify  $M$ -set multivariate functions  $Y_1, \dots, Y_M$ . For each set  $m$ , the mean functions of different groups are assumed to be similar. In EEG recordings,  $M$  can be considered as the number of channels,  $t$  is the time argument of epochs, and  $k$  is the index of epoch.

Define the second moment and cross second moment as

$$c_{g,m_1m_2}(t, s) = E \left( X_{km_1}^{(g)}(t) X_{km_2}^{(g)}(s) \right), \quad m_1, m_2 = 1, \dots, M,$$

and the estimator of  $c_{g,m_1m_2}(t, s)$  is

$$\hat{c}_{g,m_1m_2}(t, s) = \frac{1}{n_g} \sum_{k=1}^{n_g} X_{km_1}^{(g)}(t) X_{km_2}^{(g)}(s), \quad m_1, m_2 = 1, \dots, M.$$

We propose to compare the weighted concatenated second moment functions, defined as

$$S_g(t, s) = \begin{pmatrix} \omega^2(1)c_{11}^{(g)} & \omega(1)\omega(2)c_{12}^{(g)} & \cdots & \omega(1)\omega(M)c_{1M}^{(g)} \\ \omega(1)\omega(2)c_{21}^{(g)} & \omega^2(2)c_{22}^{(g)} & \cdots & \omega(2)\omega(M)c_{2M}^{(g)} \\ \vdots & \vdots & \ddots & \vdots \\ \omega(1)\omega(M)c_{M1}^{(g)} & \omega(2)\omega(M)c_{M2}^{(g)} & \cdots & \omega^2(M)c_{MM}^{(g)} \end{pmatrix},$$

where the weight  $\omega(m)$  should depend on the discrepancy of the  $m$ th set of functions. Then by the same argument, the basis function used for the comparison of the concatenated second moment should capture the main discrepancy

$$\|\mathcal{C}_0(x) - \mathcal{C}_1(x)\|_S,$$

where  $C_g(x) = \int S_g(t, s)x(s)ds$ . Therefore, we propose to use the eigenfunctions of  $\mathcal{C} = (\mathcal{C}_0 - \mathcal{C}_1)^2$  to compute the distance. The classification procedure is summarized in Algorithm 2.

---

**Algorithm 2** Classification algorithm for multivariate functions

---

**Step 1.** Fix  $d$ , obtain the eigenfunction of  $\hat{\mathcal{C}} = (\hat{\mathcal{C}}_0 - \hat{\mathcal{C}}_1)^2$ , denoted by,  $\{\hat{\psi}_j\}_{j=1}^d$ , where

$$\hat{\psi}_j = (\hat{\psi}_{j1}|\hat{\psi}_{j2}|\cdots|\hat{\psi}_{jM}).$$

**Step 2.** Then compute the scores  $\hat{\mathcal{S}}_{ij} = \langle \mathcal{Y}(\hat{\psi}_i), \hat{\psi}_j \rangle$  for  $i, j = 1, \dots, d$ , where

$$\mathcal{Y} = (\omega(1)Y_1 | \dots | \omega(M)Y_M)$$

is the weighted concatenated function.

**Step 3.** Compute  $\hat{D}_g = \sum_{i,j}^d (\hat{\mathcal{S}}_{ij} - \langle \hat{\mathcal{C}}_g(\hat{\psi}_i), \hat{\psi}_j \rangle)^2$ . If  $\hat{D}_0 - \hat{D}_1 < 0$ , jointly classify  $Y_1, \dots, Y_M$  to  $\Pi_0$ , otherwise, classify them to  $\Pi_1$ .

---

In this case, the discrepancy and variability come from multiple sources. We stress that if at least for one set of functions, the discrepancy between the two groups goes to infinity, and the variability of the scores do not go to infinity very fast, then we can get perfect classification. The result is illustrated in Theorem 2.

**Theorem 2.** Assume  $\|\mathcal{C}_0 - \mathcal{C}_1\|_S > 0$  and  $E\|Y^4\| < \infty$ , the misclassification probability  $P(\Pi_{1-g}|\Pi_g)$  satisfies

$$P(\Pi_{1-g}|\Pi_g) \leq \frac{4M^2 \sum_{i,j=1}^d \sum_{m_1, m_2} \sigma_{m_1 m_2, ij}^{(g)}}{\sum_{i,j=1}^d \langle (\mathcal{C}_0 - \mathcal{C}_1)\psi_i, \psi_j \rangle^2},$$

where  $\sigma_{m_1 m_2, ij}^{(g)} = \omega^2(m_1)\omega^2(m_2)\text{var}(\langle Y_{m_1}, \psi_{im_1} \rangle \langle Y_{m_2}, \psi_{jm_2} \rangle)$ .

**Remark:** The value of weight function  $\omega(m)$  is large if we can discriminate the  $m$ th set of functions well. For examples, assume  $f(\cdot)$  is a increasing function, then we can set  $\omega(m) = f(\sum_{g=0}^1 P_m(\Pi_{1-g}|\Pi_g))$  or  $\omega(m) = f(\|\hat{\mathcal{C}}_{0,mm} - \hat{\mathcal{C}}_{1,mm}\|_S)$ , where  $P_m(\Pi_{1-g}|\Pi_g)$  is the probability of misclassifying an object in group  $g$  into group  $1 - g$  based on the  $m$ th set only, which can be estimated by a cross-validation procedure.

### 3.4 Correlated functional data

When functions are not independent, we may further compare  $C_g^{(h)}$  with  $h > 0$ . Assume  $(X_k^{(g)}(t) : k \in \mathbb{N}_+)$  are correlated across  $k$ , and we collect a sequence of sample consecutively  $(Y_k(t) : k = 1, \dots, p+1)$ , where  $p+1$  is number of samples to be jointly classified. One way to do joint classification is to apply the technique proposed for multivariate functional data. Since correlation across curves usually decay very fast, the correlation between concatenated functions should be less pronounced. However, if the second moment structure of two groups are only different in the auto second moment at some specific, rather than all, lags, it is not helpful to consider the second moments at lags where no discrepancy is present. Here we propose another method, which check the auto second moment functions separately.

The estimators of  $C_g^{(h)}(x)$  and  $C_g^{(-h)}(x)$  are respectively

$$\hat{C}_g^{(h)}(x) = \int \frac{1}{n_g - h} \sum_{k=1}^{n_g-h} X_k^{(g)}(t) X_{k+h}^{(g)}(s) x(s) ds,$$

$$\hat{C}_g^{(-h)}(x) = \int \frac{1}{n_g - h} \sum_{k=1}^{n_g-h} X_{k+h}^{(g)}(t) X_k^{(g)}(s) x(s) ds.$$

We propose to compare the operators  $C_g^{(h)} + C_g^{(-h)}$ ,  $g = 0, 1$ ,  $h = 1, \dots, p$ . The basis function used for comparison of second moments should capture most of the discrepancy

$$\|C_0^{(h)} + C_0^{(-h)} - (C_1^{(h)} + C_1^{(-h)})\|_{\mathcal{S}}.$$

Similar with the independent case, we note that the first few eigenfunctions of  $(C_0^{(h)} + C_0^{(-h)} - (C_1^{(h)} + C_1^{(-h)}))^2$  account for most of the above discrepancy, and in order to find the most important eigenfunctions, we apply fPCA to the operator

$$\mathcal{R}_h = (C_0^{(h)} + C_0^{(-h)} - (C_1^{(h)} + C_1^{(-h)}))^2,$$

which is symmetric and positive definite, and employ the first  $d$  eigenfunctions for comparison.

In practice, we can only consider finite lags. Suppose we consider the comparison up to lag  $p$ , we need to consecutively collect  $p + 1$  functions for each group, i.e.  $Y_1, \dots, Y_{p+1}$ , and classify them jointly. Let

$$\kappa_g^{(h)} = C_g^{(h)} + C_g^{(-h)}$$

and

$$\begin{aligned} \hat{\kappa}_{y,h}(x) &= \frac{1}{p+1-h} \sum_{k=1}^{p+1-h} Y_k \langle Y_{k+h}, x \rangle \\ &+ \frac{1}{p+1-h} \sum_{k=1}^{p+1-h} Y_{k+h} \langle Y_k, x \rangle, \end{aligned}$$

The second moments at different lags usually have different contributions to classification, so we consider the weighted classifier, the procedure is summarized in Algorithm 3.

---

**Algorithm 3** Classification algorithm for correlated functions

---

**Step 1.** Fix  $d_h$ , obtain the eigenfunction of  $\hat{\mathcal{R}}_h$ ,  $h = 1, \dots, p$ , say,  $(\hat{\nu}_{h,j} : j = 1, \dots, d_h)$ .

**Step 2.** Then compute the scores  $\hat{S}_{g,ij}^h = \langle \hat{\kappa}_g^{(h)}(\hat{\nu}_{h,i}), \hat{\nu}_{h,j} \rangle$  for  $i, j = 1, \dots, d_h$ .

**Step 3.** Compute

$$\hat{D}_g = \sum_{h=1}^p W(h) \sum_{i,j=1}^{d_h} (\hat{S}_{g,ij}^h - \langle \hat{\kappa}_{y,h}(\hat{\nu}_{h,i}), \hat{\nu}_{h,j} \rangle)^2.$$

If  $\hat{D}_0 - \hat{D}_1 < 0$ , classify  $Y_1, \dots, Y_{p+1}$  to  $\Pi_0$ , otherwise, classify them to  $\Pi_1$ .

---

When the functions are correlated, we need to select the the best lags so that the second moment functions are significantly different. When sample size is limited, we propose to apply Monte-Carlo cross-validation procedure (see e.g. Xu & Liang (2001)). In each

step, we randomly separate the sample into two sets, say, training set and testing set. We classify the objects in the testing set based on  $\hat{\kappa}_g^{(h)}(x)$  only, which is estimated from the training set, and then obtain the misclassification rate. We can repeat the same procedure for multiple times and if the average misclassification rate does not exceed a pre-specified threshold, then we incorporate the corresponding  $\kappa_g^{(h)}(x)$  into classification.

The major contribution of Theorem 3 is showing that the classification is perfect if, at least for one lag  $h$ , the second moment discrepancy goes to infinity, and the variability, which comes from  $\hat{\kappa}_{y,h}$  at multiple lags, is not very large.

**Theorem 3.** Assume  $\sum_{h=0}^p \|\kappa_0^{(h)} - \kappa_1^{(h)}\|_S > 0$  and  $E\|Y_k^4\| < \infty$ , and the weight function  $W(\cdot)$  satisfies  $\tau_1 \leq W(\cdot) \leq \tau_2$ , where  $\tau_1, \tau_2$  are two positive constants, the misclassification probability  $P(\Pi_{1-g}|\Pi_g)$  satisfies

$$P(\Pi_{1-g}|\Pi_g) \leq \frac{4\mathcal{T}pE \left\{ \max_h \left( \sum_{i,j=1}^{d_h} \langle (\hat{\kappa}_{y,h} - \kappa_g^{(h)})(\nu_{h,i}), \nu_{h,j} \rangle^2 \right) \right\}}{\sum_{h=0}^p \sum_{i,j=1}^{d_h} \langle (\kappa_0^{(h)} - \kappa_1^{(h)})(\nu_{h,i}), \nu_{h,j} \rangle^2},$$

where  $\mathcal{T}$  is a constant determined by  $\tau_1$  and  $\tau_2$ .

**Remark:** We should set a large value to  $W(h)$  if we can discriminate  $\kappa_0^{(h)}(t, s)$  and  $\kappa_1^{(h)}(t, s)$  well. We can apply cross-validation to obtain the classification rate  $p(h)$  based on  $\hat{\kappa}_{y,h}$  only, and set  $W(h) = g(p(h))$ , where  $g(\cdot)$  is an increasing function. In simulation, as the discrepancy at one lag is more pronounced than other lags, we find that the following weight function works well

$$W_o(h) = \begin{cases} 1, & \text{if } p(h) = \max_{h'} p(h') \\ 0, & \text{otherwise} \end{cases}$$

When the functions can be discriminated equally well at multiple lags, we need to put equal weights for those lags.



In Theorem 4, we show the consistency of the estimators. The consistency property also holds in the previous two cases.

**Theorem 4.** Suppose  $(X_k^{(g)} : k \in \mathbb{N}) \in L^4([0, 1])$  is an  $L^4 - m$ -approximable sequence (see e.g. Hörmann et al. (2010)), we have

$$E \left\{ \|(\hat{\kappa}_0^{(h)} - \hat{\kappa}_1^{(h)})^2 - (\kappa_0^{(h)} - \kappa_1^{(h)})^2\|_S \right\} \rightarrow 0$$

as  $n_0, n_1 \rightarrow \infty$ .

**Remark:** According to lemma 2.2 and 2.3 in Horváth & Kokoszka (2012), we can conclude from Theorem 4 that the estimated eigenvalues are consistent, and the estimated eigenfunctions are consistent up to a constant sign. Under independence, the sequence will be naturally  $L^4 - m$ -approximable.

### 3.5 Classification among multiple groups

Assume we have  $G$  groups  $\Pi_1, \dots, \Pi_G$ , where  $G > 2$ , the procedure can be naturally extended to this case. In such case, we can do pairwise classification for different pairs of groups. More specifically, We first compare the first two groups  $\Pi_1$  and  $\Pi_2$ , if the new object  $Y$  is classified into  $\Pi_1$ , then we further do pairwise comparison between  $\Pi_1$  and  $\Pi_3$ . We can repeat the comparison until we find the group whose centroid is the closest to  $Y$ . The classification algorithm for multi-group independent functions is summarized in Algorithm 4.

**Remark:** We only discuss the extension in independent case, however, the algorithm can be extended in the cases of multivariate and correlated functions in a similar way.

---

**Algorithm 4** Classification algorithm for multiple groups

---

- 1: **Set**  $i = 1$ .
- 2: **for**  $j$  **in**  $(i + 1) : G$  **do**
- 3:     **Fix**  $d_{ij}$ , and obtain the eigenfunction of  $(\hat{C}_i^0 - \hat{C}_j^0)^2$ , say,

$$(\hat{\nu}_l^{ij} : l = 1, \dots, d_{ij}).$$

- 4:     Obtain the scores for the comparison between group  $i$  and  $j$ ,

$$\hat{S}_{g,ll'}^{ij} = \langle \hat{C}_g^{(0)}(\hat{\nu}_l^{ij}), \hat{\nu}_{l'}^{ij} \rangle, \quad g = i, j.$$

- 5:     Obtain the scores of the new object  $Y$ ,

$$\hat{S}_{y,ll'}^{ij} = \langle Y, \hat{\nu}_l^{ij} \rangle \langle Y, \hat{\nu}_{l'}^{ij} \rangle.$$

- 6:     **if**  $\sum_{l,l'=1}^{d_{ij}} (\hat{S}_{i,ll'}^{ij} - \hat{S}_{y,ll'}^{ij})^2 > \sum_{l,l'=1}^{d_{ij}} (\hat{S}_{j,ll'}^{ij} - \hat{S}_{y,ll'}^{ij})^2$ , **then** set  $i = j$ .
  - 7:     **end if**
  - 8: **end for**
  - 9: **return**  $i$  as the index of  $Y$ .
- 

## 4 Simulations

### 4.1 General setting

To study the finite sample property of the method, we simulated two groups ( $n_1 = n_2 = 200$ ) of independent or correlated functions in a  $D$ -dimensional space spanned by the first  $D$  Fourier basis or B-spline basis functions ( $D = 21$ ). The two groups have the same mean function, which were set to be zero, and different covariance functions. The functions in each group have the following expansion,

$$X_i^{(g)}(t_j) = \sum_{k=1}^D \xi_{ik}^{(g)} \phi_k(t_j) + e(t_j),$$

where  $\{\phi_k(t)\}$  are  $k$ th basis function, and  $e(t_j) \sim \mathcal{N}(0, \sigma^2)$ ,  $j = 1, 2, \dots, l$ , where  $l$  is the number of equally-spaced discrete grids, and  $\sigma^2 = 0.7$ .

## 4.2 Independent functions

For independent functions, we tried two different classes of basis functions for simulation. In the first setup, the functions were generated by 21  $B$ -spline functions. The scores of two groups follow normal distribution,

$$(\xi_k^{(g)}: k = 1, \dots, 21) \sim \mathcal{N}(0, \sigma_g^b).$$

$\sigma_1^b$  and  $\sigma_2^b$  were generated in two steps: First set

$$\sigma_1^b = I_3 \otimes \text{diag}(a, a, b, b, b, a, a), \quad \sigma_2^b = I_3 \otimes \text{diag}(b, b, a, a, a, b, b),$$

and  $I_3$  is a  $3 \times 3$  identity matrix, then replaced the first and last element of  $\sigma_1^b$  and  $\sigma_2^b$  with zero to avoid boundary effect. In the other setup, the functions were generated by 21 Fourier functions. The scores of two groups follow the same normal distribution. For different pairs of  $a, b$ , we compared four methods: 1) our new method (SMFC); 2) projection method (denoted by PJ, Chiou & Li (2007)); 3) functional linear classifier (denoted by FLC, Delaigle & Hall (2012)); 4) functional quadratic classifier (denoted by FQC, Delaigle & Hall (2013)).

We simulated 200 curves for each group, and classified 100 curves by the other 100 curves. We repeated the classification procedure 100 times and calculated the average classification rates (ACR) for each group, which are presented in Table 1,2.

In the simulation, we can see that, even though the projection method and the functional quadratic classifier also check the second moment structure, sometimes they still cannot distinguish groups with different second moments. That is because, in those methods, we compare groups using the group-wise principal components, which are not guaranteed to capture the discrepancy. Comparing with those methods, we use the basis functions that account for most of the discrepancy between groups, and that makes

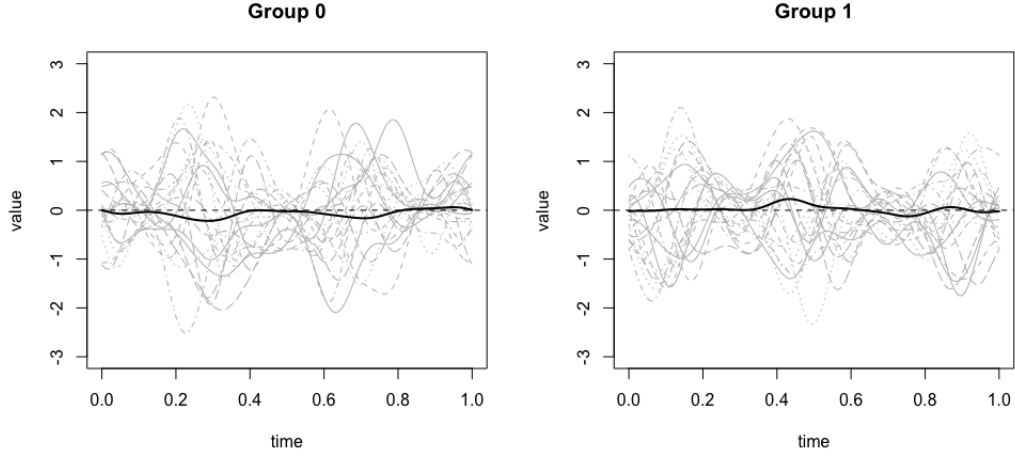


Figure 2: The functions of the two groups in the first setup ( $a = 2, b = 0.5$ )

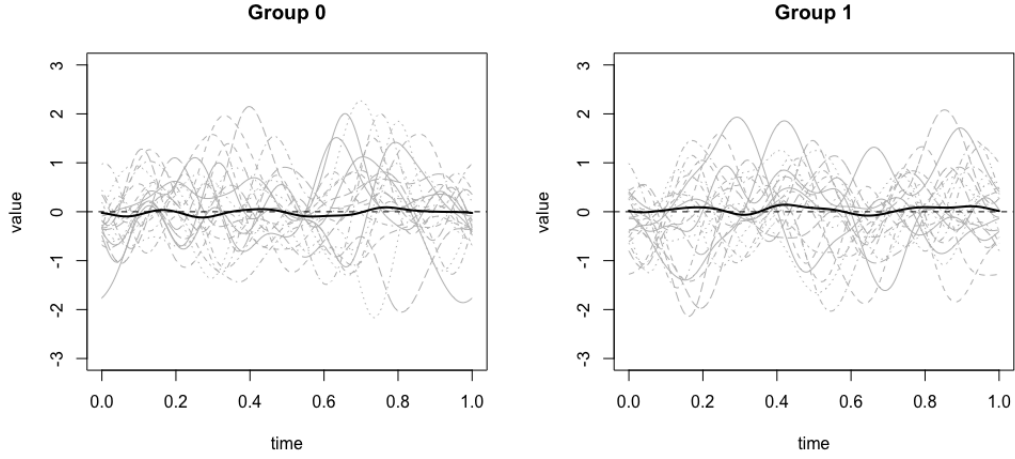


Figure 3: The functions of the two groups in the first setup ( $a = 1.5, b = 1$ )

$a = 2, b = 0.5$ (B-spline)								
Methods	SMFC		PJ		FLC		FQC	
ACR	$\Pi_0$	$\Pi_1$	$\Pi_0$	$\Pi_1$	$\Pi_0$	$\Pi_1$	$\Pi_0$	$\Pi_1$
$\Pi_0$	0.9511	0.0489	0.9668	0.0332	0.5031	0.4969	0.4264	0.5736
$\Pi_1$	0.0636	0.9364	0.0272	0.9728	0.4979	0.5021	0.7511	0.2489
$a = 1.5, b = 1$ (B-spline)								
Methods	SMFC		PJ		FLC		FQC	
ACR	$\Pi_0$	$\Pi_1$	$\Pi_0$	$\Pi_1$	$\Pi_0$	$\Pi_1$	$\Pi_0$	$\Pi_1$
$\Pi_0$	0.7109	0.2891	0.6288	0.3712	0.5024	0.4976	0.6510	0.3490
$\Pi_1$	0.2875	0.7125	0.3506	0.6494	0.4968	0.5032	0.3344	0.6656

Table 1

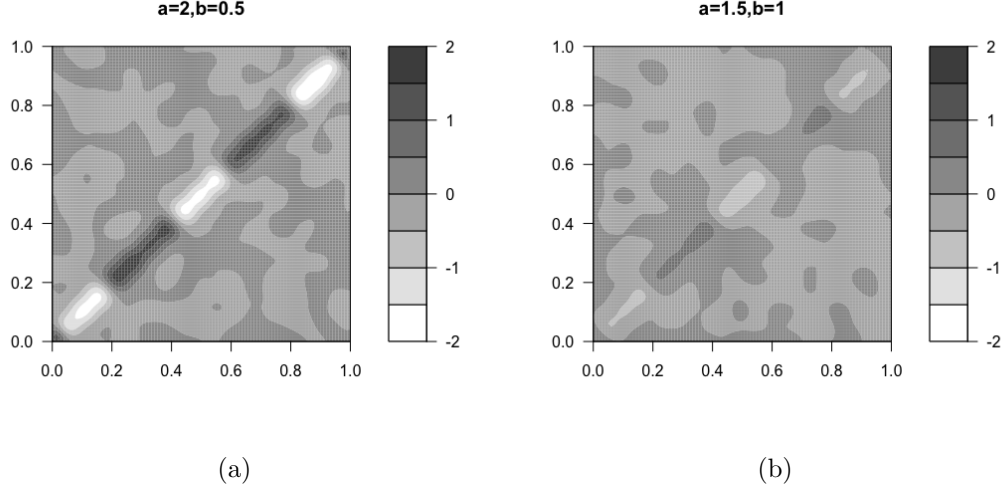


Figure 4:  $c_0^{(0)}(t, s) - c_1^{(0)}(t, s)$  contour plot (B-spline basis)

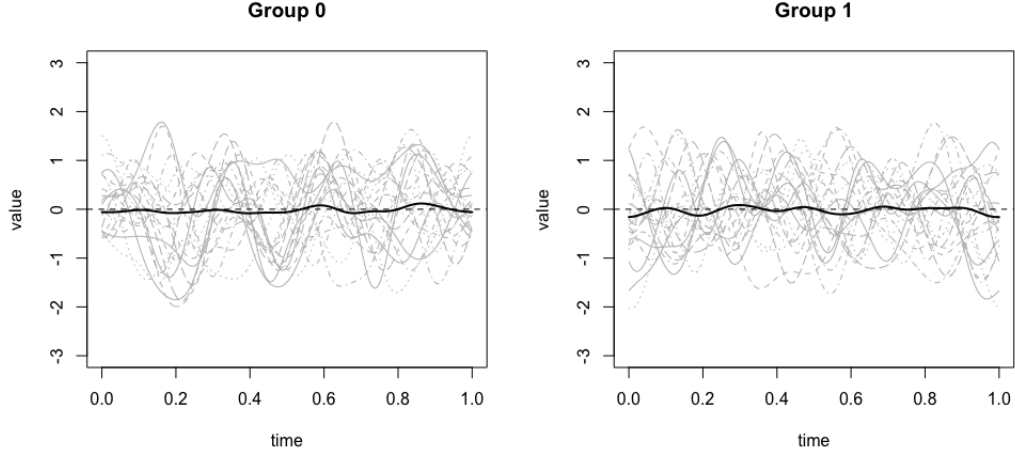


Figure 5: The functions of the two groups in the second setup ( $a = 2, b = 0.5$ )

$a = 2, b = 0.5$ (Fourier basis)								
Methods	SMFC		PJ		FLC		FQC	
ACR	$\Pi_0$	$\Pi_1$	$\Pi_0$	$\Pi_1$	$\Pi_0$	$\Pi_1$	$\Pi_0$	$\Pi_1$
$\Pi_0$	0.9974	0.0026	0.9987	0.0013	0.5040	0.4960	0.0047	0.9953
$\Pi_1$	0.0088	0.9912	0.0040	0.9960	0.4662	0.5338	0.9840	0.0160
$a = 1.5, b = 1$ (Fourier basis)								
Methods	SMFC		PJ		FLC		FQC	
ACR	$\Pi_0$	$\Pi_1$	$\Pi_0$	$\Pi_1$	$\Pi_0$	$\Pi_1$	$\Pi_0$	$\Pi_1$
$\Pi_0$	0.7813	0.2187	0.5540	0.4460	0.4971	0.5029	0.7837	0.2163
$\Pi_1$	0.2302	0.7698	0.3126	0.6874	0.4944	0.5056	0.3481	0.6519

Table 2

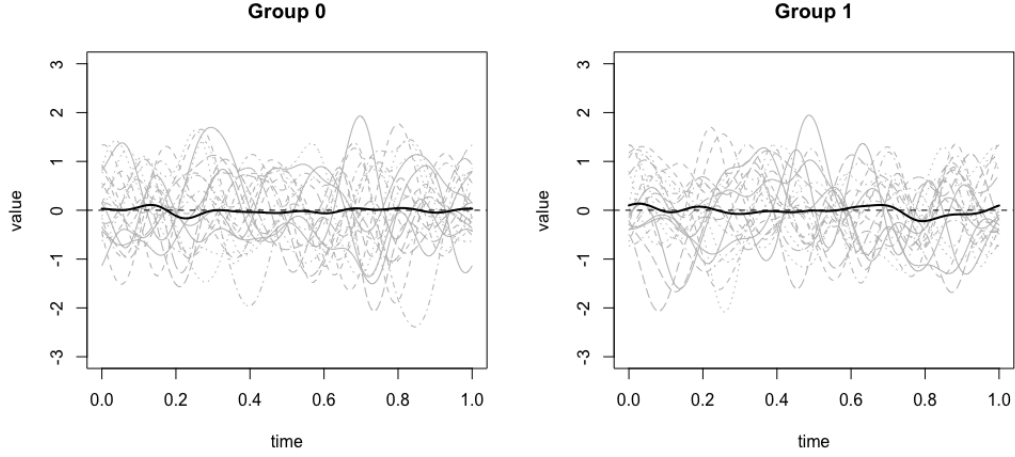


Figure 6: The functions of the two groups in the second setup ( $a = 1.5, b = 1$ )

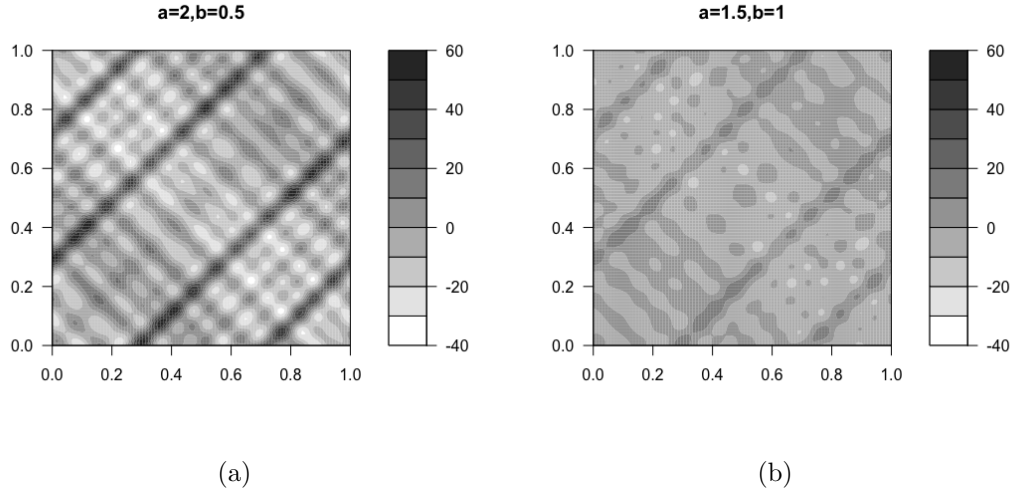


Figure 7:  $c_0^{(0)}(t, s) - c_1^{(0)}(t, s)$  contour plot (Fourier basis)

our method being able to detect the discrepancy more efficiently, especially when the difference in covariance structure is not pronounced.

### 4.3 Correlated functions

To analyze the finite sample properties of the new method in the case of correlated functional data, we discriminated a FAR(1) process and a sequence of i.i.d. random functions by the proposed method. Both sequences were generated in a 21-dimensional

sub-space spanned by the first 21 Fourier basis,  $\mathbf{F}(t) = (F_1(t), \dots, F_{21}(t))$ , where each function were generated in the same expansion as described in the previous section. The scores of the first sequence follows a VAR(1) process, i.e.

$$\xi_i^{(1)} = A\xi_{i-1}^{(1)} + \epsilon_i,$$

where  $\epsilon_i$  is i.i.d. 21-dimensional random error vectors following  $\mathcal{N}(0, \Sigma_1)$ , where  $\Sigma_1$  is a diagonal matrix with diagonal elements  $\sigma$ . Two types of  $\sigma$  were chosen, namely,

$$\sigma_1 = (1.2^{-D} : D = 1, \dots, 21), \quad \sigma_2 = (1/D : D = 1, \dots, 21).$$

The scores of the second sequence identically follow the normal distribution  $\mathcal{N}(0, \Sigma_2)$ .

To show the usefulness of the new method for correlated data, we simulated the two sequences such that they have similar covariance functions but different auto-covariance functions. To be specific, we set  $A = aI_{21}$ , where  $a = 0.3, 0.6, 0.9$  and  $I_{21}$  is the 21-dimensional identity matrix. Then the covariance function of the FAR(1) process should be  $(1 - a^2)^{-1}\mathbf{F}(t)\Sigma_1\mathbf{F}^T(s)$ . Then set  $\Sigma_2 = (1 - a^2)^{-1}\Sigma_1$ , consequently the covariance function of the second sequence is the same as that of the first sequence. The auto-covariance function of the two sequences at lag  $h$  ( $h = 1, 2, \dots$ ) are

$$c_h^{(0)}(t, s) = a^h(1 - a^2)^{-1}\mathbf{F}(t)\Sigma_1\mathbf{F}^T(t), \quad c_h^{(1)}(t, s) = 0.$$

We tried three weight functions  $W_1(h) = p_h$ ,  $W_2(h) = (p_h)^2$ , and  $W_o(h)$ , and compared the corresponding classification rates. 500 functions were simulated as training set, and 100 more functions were simulated as testing set. We repeated the procedure 100 times and the average classification rates are shown in Table 5–7.

**Remark:** In the simulation, weight function  $W_o(h)$  is optimal, which means we can only consider the most different second moment functions. That is because the difference

$a = 0.9, \sigma_1$						
Weight	$W_1(h)$		$W_2(h)$		$W_o(h)$	
ACR	$\Pi_0$	$\Pi_1$	$\Pi_0$	$\Pi_1$	$\Pi_0$	$\Pi_1$
$\Pi_0$	0.8664	0.1336	0.8830	0.117	0.9620	0.038
$\Pi_1$	0.0236	0.9764	0.0214	0.9786	0.0486	0.9514

$a = 0.9, \sigma_2$						
Weight	$W_1(h)$		$W_2(h)$		$W_o(h)$	
ACR	$\Pi_0$	$\Pi_1$	$\Pi_0$	$\Pi_1$	$\Pi_0$	$\Pi_1$
$\Pi_0$	0.6940	0.3060	0.7010	0.2990	0.8056	0.1944
$\Pi_1$	0.0832	0.9168	0.0786	0.9214	0.1338	0.8662

Table 3

$a = 0.6, \sigma_1$						
Weight	$W_1(h)$		$W_2(h)$		$W_o(h)$	
ACR	$\Pi_0$	$\Pi_1$	$\Pi_0$	$\Pi_1$	$\Pi_0$	$\Pi_1$
$\Pi_0$	0.6558	0.3442	0.6902	0.3098	0.8122	0.1878
$\Pi_1$	0.0798	0.9202	0.0754	0.9246	0.0964	0.9036

$a = 0.6, \sigma_2$						
Weight	$W_1(h)$		$W_2(h)$		$W_o(h)$	
ACR	$\Pi_0$	$\Pi_1$	$\Pi_0$	$\Pi_1$	$\Pi_0$	$\Pi_1$
$\Pi_0$	0.6538	0.3462	0.6776	0.3224	0.7570	0.2430
$\Pi_1$	0.1618	0.8382	0.1632	0.8368	0.1984	0.8016

Table 4

$a = 0.3, \sigma_1$						
Weight	$W_1(h)$		$W_2(h)$		$W_o(h)$	
ACR	$\Pi_0$	$\Pi_1$	$\Pi_0$	$\Pi_1$	$\Pi_0$	$\Pi_1$
$\Pi_0$	0.5520	0.4480	0.5678	0.4322	0.6406	0.3594
$\Pi_1$	0.2552	0.7448	0.2334	0.7666	0.2394	0.7606

$a = 0.3, \sigma_2$						
Weight	$W_1(h)$		$W_2(h)$		$W_o(h)$	
ACR	$\Pi_0$	$\Pi_1$	$\Pi_0$	$\Pi_1$	$\Pi_0$	$\Pi_1$
$\Pi_0$	0.5842	0.4158	0.5848	0.4152	0.6410	0.3590
$\Pi_1$	0.3718	0.6282	0.3592	0.6408	0.3844	0.6156

Table 5

of the second moment decays exponentially fast. However, when the second moments of some lags are equally different between groups, we need to compare all of them, and in that case,  $W_1(h)$  and  $W_2(h)$  should be better than  $W_o(h)$ . The asymmetry of misclassification comes from the unequal variability of  $\hat{\kappa}_{y,h}$  in different groups.



## 5 Real data analysis

### 5.1 Phoneme log-periodograms

We applied our method to the digitized speech phoneme trajectories. The dataset were described in Hastie et al. (2009) and are available from [www-stat.stanford.edu/ElemStatLearn](http://www-stat.stanford.edu/ElemStatLearn). In the dataset, we have log-periodograms constructed from 32 ms recordings of males pronouncing five different phonemes. The two groups to be discriminated are the trajectories of phoneme ‘aa’ as in ‘dark’ and ‘ao’ as in ‘water’. In Figure 8, we see that the mean functions of log-periodograms are difficult to be distinguished from each other. The sample sizes are respectively  $n_0 = 695$  and  $n_1 = 1022$ , and each function was observed at 256 equispaced frequencies. The trajectories were smoothed with 31 B-spline functions.

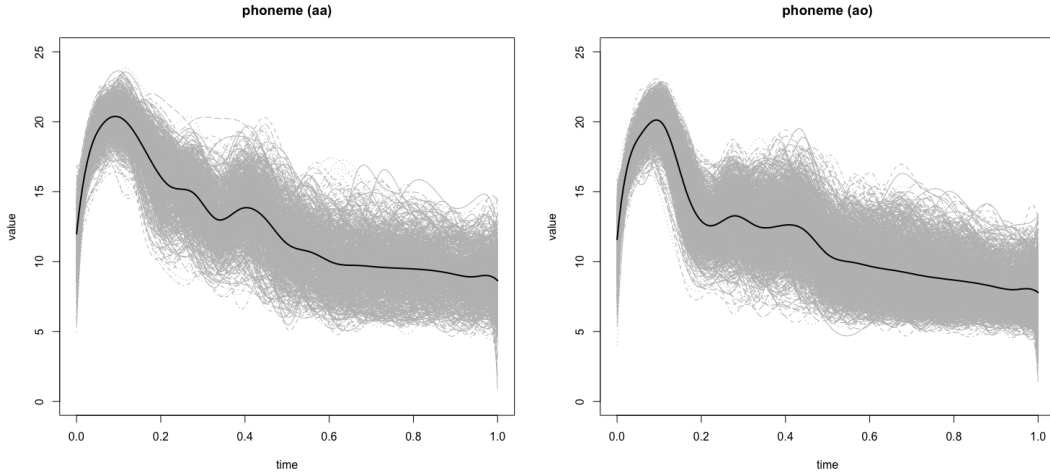


Figure 8: Phoneme log-periodogram curves for ‘aa’ and ‘ao’

We applied the Monte-Carlo cross validation procedure to estimate the classification rate. In each run, we randomly selected 500 curves from each group for training data, and 100 curves for testing data. We repeated the procedure for 100 simulation runs, and computed the averaged classification rate shown in Table 6, and the estimated distribution of the classification rate of the four methods are displayed in Figure 9. By

comparison, the functional linear classifier (Delaigle & Hall (2012)) worked well, and our method was also very competitive to other methods.

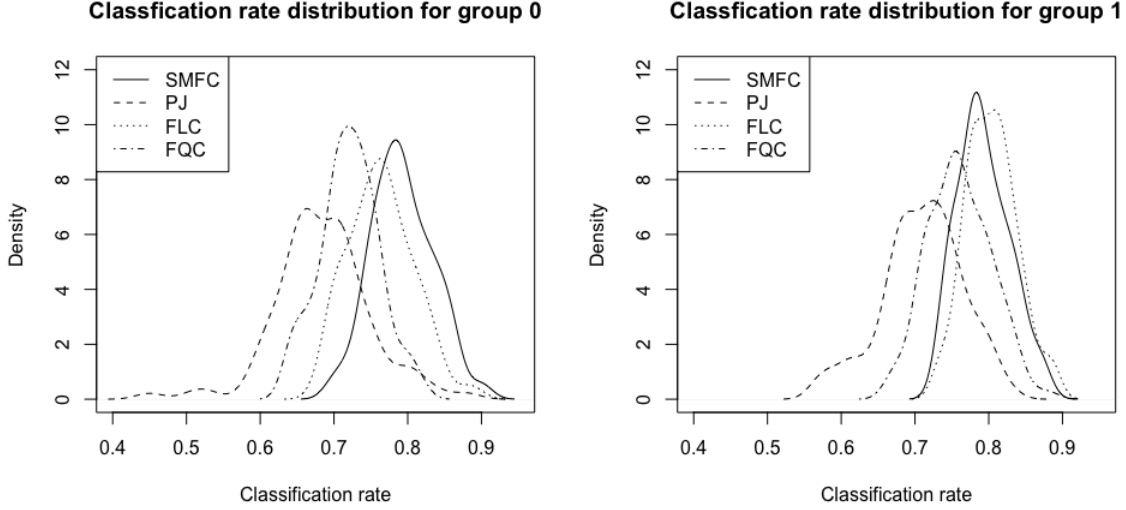


Figure 9

Methods	SMFC		PJ		FLC		FQC	
ACR	$\Pi_0$	$\Pi_1$	$\Pi_0$	$\Pi_1$	$\Pi_0$	$\Pi_1$	$\Pi_0$	$\Pi_1$
$\Pi_0$	0.7951	0.2049	0.6854	0.3146	0.7653	0.2347	0.7325	0.2675
$\Pi_1$	0.2109	0.7891	0.3017	0.6983	0.1926	0.8074	0.2445	0.7555

Table 6

## 5.2 Brain activity

Consider an experimental setting where multichannel brain signals are recorded continuously from an animal (rat, monkey, human) over a certain period of time. One important feature of these electroencephalogram recordings is that the means of each epoch are always zero. Therefore we cannot distinguish different states of brain from the mean difference of EEG recordings. We applied our method in discriminating local field potential (LFP) of rats based on the experimentation of Frostig and Wann (see e.g. Wann (2017)). Microelectrodes were inserted in 32 locations on the rat cortex. From these microelectrodes,  $T = 1000$  time points were recorded per second. As we

assume a stationary behavior within each second, we considered each second as a distinct epoch. A total of  $r = 600$  epochs were recorded. Midway in this period (at epoch  $r = 300$ ), stroke was mechanically induced on each rat. We applied signal filtering on each epoch and use the filtered trajectories in  $\delta$ -frequency band for classification, which are displayed in Figure 10. We employed our method to discriminate the rat brain activity before and after the stroke.

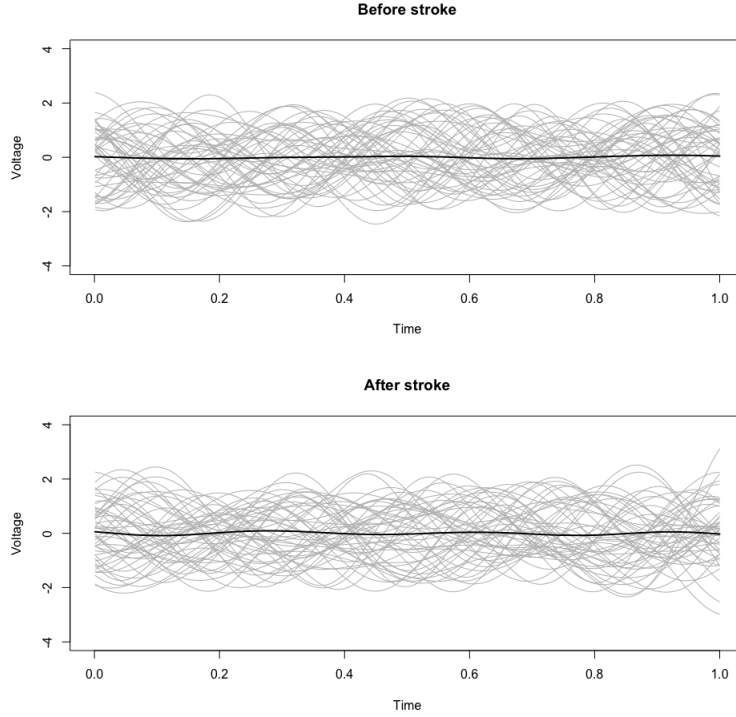


Figure 10: Scaled EEG recordings ( $\delta$ -frequency band) before and after the stroke. Black curves represent the mean functions.

We found that the two groups present the second moment discrepancy mainly at lag 0, and thus we did not consider other lags. We concatenated the weighted second moment and cross second moment functions, which were computed as

$$\hat{C}_{g,ij}^{\omega}(t,s) = \omega(i)\omega(j) \times \frac{1}{200} \sum_{k=1}^{200} (X_k^{gi}(t), X_k^{gj}(s)), \quad i, j = 1, \dots, 32,$$

to obtain kernel  $\hat{\mathcal{C}}_0$  and  $\hat{\mathcal{C}}_1$ . Figure 11 in appendix presents the first five functional principal components of  $(\hat{\mathcal{C}}_0 - \hat{\mathcal{C}}_1)^2(t,s)$ . Figure 12 in appendix presents the corresponding

average scores of the two groups.

We obtained the weight  $\omega(i)$ ,  $i = 1, \dots, 32$ , by Monte-Carlo cross validation. Among the first 200 curves, we randomly selected 100 curves as training data, and 30 curves as testing data, and classified the testing data by comparing each individual channel, then obtained the corresponding classification rate. We repeated the process 50 times and computed the average classification rate for each channel and used those values as  $\omega(i)$ ,  $i = 1, \dots, 32$ . Then we used the first 200 functions to classify the rest 100 functions by comparing the concatenated second moment functions. The classification rate of  $\Pi_0$  is 0.93, and for  $\Pi_1$ , we can achieve perfect classification.

To make the comparison fair, we concatenated the functions of different channel for other three competitor methods, and Chiou's projection method also worked competitively, but other methods cannot discriminate the different groups in this case.

## 6 Conclusion

We developed a new classification method for functional data, in the case that different groups have similar mean functions. We proposed to compare the second moment functions of the scaled trajectories. The comparison is constrained in the sub-space spanned by the feature functions that account for most of the discrepancy of the second moment functions. The classification performance is influenced by two factors: 1) discrepancy between groups and 2) variability of the objects to be classified. The dimension reduction technique will remove the unnecessary variability, which only explain variance for each individual group, but do not explain the difference between groups. The classification procedure is also extended to multivariate functional data and correlated functional data. We have shown that, as the discrepancy of the second moment functions goes to infinity, this second moment based functional classifier will become perfect. This

method checks only the second moment discrepancy, but similar framework can be established for the comparison of higher order moment functions. The estimation and dimension reduction of higher order moment functions is not straightforward and we do not pursue it here. Furthermore, when the sequences are not stationary, which means the second moments vary across time, we can develop non-stationary framework based on the stationary framework we developed in this paper.

## References

- Anderson, T. W., Bahadur, R. R. et al. (1962), ‘Classification into two multivariate normal distributions with different covariance matrices’, *The annals of mathematical statistics* **33**(2), 420–431.
- Barachant, A., Bonnet, S., Congedo, M. & Jutten, C. (2013), ‘Classification of covariance matrices using a riemannian-based kernel for bci applications’, *Neurocomputing* **112**, 172–178.
- Biau, G., Bunea, F. & Wegkamp, M. H. (2005), ‘Functional classification in hilbert spaces’, *IEEE Transactions on Information Theory* **51**(6), 2163–2172.
- Chiou, J.-M. & Li, P.-L. (2007), ‘Functional clustering and identifying substructures of longitudinal data’, *Journal of the Royal Statistical Society: Series B (Statistical Methodology)* **69**(4), 679–699.
- Chiou, J.-M. & Li, P.-L. (2008), ‘Correlation-based functional clustering via subspace projection’, *Journal of the American Statistical Association* **103**(484), 1684–1692.
- Delaigle, A. & Hall, P. (2012), ‘Achieving near perfect classification for functional data’, *Journal of the Royal Statistical Society: Series B (Statistical Methodology)* **74**(2), 267–286.

- Delaigle, A. & Hall, P. (2013), ‘Classification using censored functional data’, *Journal of the American Statistical Association* **108**(504), 1269–1283.
- Farquhar, J. (2009), ‘A linear feature space for simultaneous learning of spatio-spectral filters in bci’, *Neural Networks* **22**(9), 1278–1285.
- Fehr, D., Beksi, W. J., Zermas, D. & Papanikolopoulos, N. (2014), Rgb-d object classification using covariance descriptors, *in* ‘2014 IEEE International Conference on Robotics and Automation (ICRA)’, IEEE, pp. 5467–5472.
- Fehr, D., Cherian, A., Sivalingam, R., Nickolay, S., Morellas, V. & Papanikolopoulos, N. (2012), Compact covariance descriptors in 3d point clouds for object recognition, *in* ‘2012 IEEE International Conference on Robotics and Automation’, IEEE, pp. 1793–1798.
- Fontaine, C., Frostig, R. D. & Ombao, H. (2019), ‘Modeling non-linear spectral domain dependence using copulas with applications to rat local field potentials’, *Econometrics and Statistics* .
- Fromont, M. & Tuleau, C. (2006), Functional classification with margin conditions, *in* ‘International Conference on Computational Learning Theory’, Springer, pp. 94–108.
- Fryzlewicz, P. & Ombao, H. (2009), ‘Consistent classification of nonstationary time series using stochastic wavelet representations’, *Journal of the American Statistical Association* **104**(485), 299–312.
- Hastie, T., Tibshirani, R. & Friedman, J. (2009), *The elements of statistical learning: data mining, inference, and prediction*, Springer Science & Business Media.
- Hoffbeck, J. P. & Landgrebe, D. A. (1996), ‘Covariance matrix estimation and classification with limited training data’, *IEEE Transactions on Pattern Analysis and Machine Intelligence* **18**(7), 763–767.

- Hörmann, S., Kokoszka, P. et al. (2010), ‘Weakly dependent functional data’, *The Annals of Statistics* **38**(3), 1845–1884.
- Horváth, L. & Kokoszka, P. (2012), *Inference for functional data with applications*, Vol. 200, Springer Science & Business Media.
- Ieva, F., Paganoni, A. M. & Tarabelloni, N. (2016), ‘Covariance-based clustering in multivariate and functional data analysis’, *The Journal of Machine Learning Research* **17**(1), 4985–5005.
- James, G. M. & Hastie, T. J. (2001), ‘Functional linear discriminant analysis for irregularly sampled curves’, *Journal of the Royal Statistical Society: Series B (Statistical Methodology)* **63**(3), 533–550.
- James, G. M. & Sugar, C. A. (2003), ‘Clustering for sparsely sampled functional data’, *Journal of the American Statistical Association* **98**(462), 397–408.
- Kluckner, S. & Bischof, H. (2009), Semantic classification by covariance descriptors within a randomized forest, *in* ‘2009 IEEE 12th International Conference on Computer Vision Workshops, ICCV Workshops’, IEEE, pp. 665–672.
- Leng, X. & Müller, H.-G. (2006), ‘Classification using functional data analysis for temporal gene expression data’, *Bioinformatics* **22**(1), 68–76.
- Li, X., Ghosal, S. et al. (2018), ‘Bayesian classification of multiclass functional data’, *Electronic Journal of Statistics* **12**(2), 4669–4696.
- Madiraju, S. V. & Liu, C.-C. (1994), Rotation invariant texture classification using covariance, *in* ‘Proceedings of 1st International Conference on Image Processing’, Vol. 2, IEEE, pp. 655–659.
- Müller, H.-G., Stadtmüller, U. et al. (2005), ‘Generalized functional linear models’, *the Annals of Statistics* **33**(2), 774–805.

- Pigoli, D., Aston, J. A., Dryden, I. L. & Secchi, P. (2014), ‘Distances and inference for covariance operators’, *Biometrika* **101**(2), 409–422.
- Preda, C., Saporta, G. & Lévêder, C. (2007), ‘Pls classification of functional data’, *Computational Statistics* **22**(2), 223–235.
- Ramsay, J. O. (2004), ‘Functional data analysis’, *Encyclopedia of Statistical Sciences* **4**.
- Sundararajan, R. R., Frostig, R. D. & Ombao, H. (2019), ‘Modeling spectral properties in stationary processes of varying dimensions with applications to brain local field potential signals’, *arXiv preprint arXiv:1911.12295* .
- Tian, T. S. & James, G. M. (2013), ‘Interpretable dimension reduction for classifying functional data’, *Computational Statistics & Data Analysis* **57**(1), 282–296.
- Wang, J.-L., Chiou, J.-M. & Müller, H.-G. (2016), ‘Functional data analysis’, *Annual Review of Statistics and Its Application* **3**, 257–295.
- Wang, X., Ray, S. & Mallick, B. K. (2007), ‘Bayesian curve classification using wavelets’, *Journal of the American Statistical Association* **102**(479), 962–973.
- Wann, E. G. (2017), Large-scale spatiotemporal neuronal activity dynamics predict cortical viability in a rodent model of ischemic stroke, PhD thesis, UC Irvine.
- Xu, Q.-S. & Liang, Y.-Z. (2001), ‘Monte carlo cross validation’, *Chemometrics and Intelligent Laboratory Systems* **56**(1), 1–11.



## A Technical proofs

*Proof of Theorem 1.* Let  $y_{ij} = \langle Y(t), \nu_i \rangle \langle Y(s), \nu_j \rangle$ , where  $(\nu_i : i \in \mathbb{N}_+)$  are the eigenfunctions of  $(C_0^{(0)} - C_0^{(1)})^2$ , we note that

$$\begin{aligned} D_0 - D_1 &= \sum_{i,j=1}^d \langle C_0^{(0)}(\nu_i) - Y \langle Y, \nu_i \rangle, \nu_j \rangle^2 - \sum_{i,j=1}^d \langle C_1^{(0)}(\nu_i) - Y \langle Y, \nu_i \rangle, \nu_j \rangle^2 \\ &= -2 \sum_{i,j=1}^d (y_{ij} - \langle C_0^{(0)} \nu_i, \nu_j \rangle) \langle (C_0^{(0)} - C_1^{(0)}) \nu_i, \nu_j \rangle - \sum_{i,j=1}^d \langle (C_0^{(0)} - C_1^{(0)}) \nu_i, \nu_j \rangle^2 \\ &= Z - t, \end{aligned}$$

where  $t = \sum_{j=1}^d \lambda_j^C$ , and  $\lambda_j^C$  is the  $j$ th eigenvalue of  $(C_0^{(0)} - C_1^{(0)})^2$ . By Chebyshev inequality, we have

$$P(D_0 > D_1) \leq E(Z^2)/t^2$$

We now seek a bound for  $E(Z^2)$ . Assume  $Y$  is from  $\Pi_0$ , then we have  $E(y_{ij}) = \langle C_0^{(0)}(\nu_i), \nu_j \rangle$ , consequently,

$$\begin{aligned} \frac{1}{4} E(Z^2) &= E \left\{ \sum_{i,j=1}^d (y_{ij} - \langle C_0^{(0)}(\nu_i), \nu_j \rangle) (\langle C_0^{(0)}(\nu_i), \nu_j \rangle - \langle C_1^{(0)}(\nu_i), \nu_j \rangle) \right\}^2 \\ &= E \left\{ \sum_{i,j=1}^d (y_{ij} - E y_{ij}) (\langle C_0^{(0)} \nu_i, \nu_j \rangle - \langle C_1^{(0)} \nu_i, \nu_j \rangle) \right\}^2, \end{aligned}$$

and by Cauchy-Schwarz inequality, we have

$$\frac{1}{4} E(Z^2) \leq \sum_{i,j=1}^d E \{y_{ij} - E y_{ij}\}^2 \sum_{i,j=1}^d \langle (C_0^{(0)} - C_1^{(0)}) \nu_i, \nu_j \rangle^2 = t \sum_{i,j=1}^d \sigma_{ij}^{(1)}$$

Consequently, we have

$$P(D_0 > D_1) \leq \frac{4 \sum_{i,j=1}^d \sigma_{ij}^{(1)}}{t}.$$

□

*Proof of Theorem 2.* Define

$$\tilde{Y}_m = \omega(m)Y_m, \quad \tilde{C}_{m_1 m_2}^{(g)} = \omega(m_1)\omega(m_2)C_{m_1 m_2}^{(g)},$$

and  $y_{ij, m_1 m_2} = \langle \tilde{Y}_{m_1}, \nu_{im_1} \rangle \langle \tilde{Y}_{m_2}, \nu_{jm_2} \rangle$ , we have

$$\begin{aligned} D_0 - D_1 &= -2 \sum_{i,j} \left\{ \sum_{m_1, m_2} \left( y_{ij, m_1 m_2} - \langle \tilde{C}_{m_1, m_2}^{(0)}(\nu_{im_1}), \nu_{jm_2} \rangle \right) \right\} \left\langle \sum_{m_1, m_2} (\tilde{C}_{m_1 m_2}^{(0)} - \tilde{C}_{m_1 m_2}^{(1)})(\nu_{im_1}), \nu_{jm_2} \right\rangle \\ &\quad - \sum_{i,j} \left\langle \sum_{m_1, m_2} (\tilde{C}_{m_1 m_2}^{(0)} - \tilde{C}_{m_1 m_2}^{(1)}) \nu_{im_1}, \nu_{jm_2} \right\rangle^2 = Z - t. \end{aligned}$$

Then by Chebyshev inequality, we have

$$P(D_0 > D_1) \leq E(Z^2)/t^2.$$

Similarly, the upper bound of  $E(Z^2)$  can be found by Cauchy-Schwarz inequality,

$$\begin{aligned} \frac{1}{4}E(Z^2) &\leq \sum_{i,j} E \left[ \sum_{m_1, m_2} (y_{m_1 m_2, ij} - \langle \tilde{C}_{m_1 m_2}^{(0)}(\nu_{im_1}), \nu_{jm_2} \rangle) \right]^2 \\ &\quad \times \sum_{i,j} \left\langle \sum_{m_1, m_2} (\tilde{C}_{m_1 m_2}^{(0)} - \tilde{C}_{m_1 m_2}^{(1)})(\nu_{im_1}), \nu_{jm_2} \right\rangle^2 \\ &\leq \sum_{i,j} \left( M^2 \sum_{m_1, m_2} \text{Var}(y_{m_1 m_2, ij}) \right) \\ &\quad \times \sum_{i,j} \left\langle \sum_{m_1, m_2} (\tilde{C}_{m_1 m_2}^{(0)} - \tilde{C}_{m_1 m_2}^{(1)})(\nu_{im_1}), \nu_{jm_2} \right\rangle^2 \end{aligned}$$

Therefore we have

$$P(D_0 > D_1) \leq \frac{4M^2 \sum_{i,j} \sum_{m_1, m_2} \text{Var}(y_{m_1 m_2, ij})}{\sum_{i,j} \left\langle \sum_{m_1, m_2} (\tilde{C}_{m_1 m_2}^{(0)} - \tilde{C}_{m_1 m_2}^{(1)})(\nu_{im_1}), \nu_{jm_2} \right\rangle^2}$$

□

*Proof of Theorem 3.* Let  $y_{ij}^h = \langle \hat{\kappa}_{y,h}(\nu_{i,h}), \nu_{j,h} \rangle$ , and assume the sequence  $Y_1, \dots, Y_{p+1}$  are from group 1. Then we have

$$\begin{aligned}
D_0 - D_1 &= \sum_{h=1}^p W(h) \sum_{i,j=1}^{d_h} \langle (\kappa_0^{(h)} - \hat{\kappa}_{y,h}) \nu_{h,i}, \nu_{h,j} \rangle^2 \\
&\quad - \sum_{h=1}^p W(h) \sum_{i,j=1}^{d_h} \langle (\kappa_1^{(h)} - \hat{\kappa}_{y,h}) \nu_{h,i}, \nu_{h,j} \rangle^2 \\
&= \sum_{h=1}^p W(h) \left( -2 \sum_{i,j}^{d_h} (y_{ij}^h - \langle \kappa_0^{(h)}(\nu_{h,i}), \nu_{h,j} \rangle) \langle (\kappa_0^{(h)} - \kappa_1^{(h)}) \nu_{h,i}, \nu_{h,j} \rangle \right) \\
&\quad - \sum_{h=1}^p W(h) \left( \sum_{i,j=1}^{d_h} \langle (\kappa_0^{(h)} - \kappa_1^{(h)}) \nu_{h,i}, \nu_{h,j} \rangle^2 \right) \\
&= Z - t
\end{aligned}$$

By Chebyshev inequality, we have

$$P(D_0 > D_1) \leq E(Z^2)/t^2.$$

Next we need to find an upper bound for  $E(Z^2)$

$$\begin{aligned}
\frac{1}{4}E(Z^2) &\leq E \left\{ \sum_{h=1}^p W(h) \sum_{i,j=1}^{d_h} (y_{ij}^h - \langle \kappa_0^{(h)}(\nu_{h,i}), \nu_{h,j} \rangle) \langle (\kappa_0^{(h)} - \kappa_1^{(h)}) \nu_{h,i}, \nu_{h,j} \rangle \right\}^2 \\
&\leq E \left\{ \sum_{h=1}^p W(h) \left( \sum_{i,j=1}^{d_h} (y_{ij}^h - \langle \kappa_0^{(h)}(\nu_{h,i}), \nu_{h,j} \rangle)^2 \right)^{1/2} \left( \sum_{i,j=1}^{d_h} \langle (\kappa_0^{(h)} - \kappa_1^{(h)}) \nu_{h,i}, \nu_{h,j} \rangle^2 \right)^{1/2} \right\}^2 \\
&\leq pE \left\{ \max_h \left( \sum_{i,j=1}^{d_h} (y_{ij}^h - \langle \kappa_0^{(h)}(\nu_{h,i}), \nu_{h,j} \rangle)^2 \right) \right\} \\
&\quad \times \left\{ \sum_{h=1}^p W(h) \left( \sum_{i,j=1}^{d_h} \langle (\kappa_0^{(h)} - \kappa_1^{(h)}) \nu_{h,i}, \nu_{h,j} \rangle^2 \right)^{1/2} \right\}^2
\end{aligned}$$

Therefore we have

$$\begin{aligned}
P(D_0 > D_1) &\leq 4pE \left\{ \max_h \left( \sum_{i,j=1}^{d_h} (y_{ij}^h - \langle \kappa_0^{(h)}(\nu_{h,i}), \nu_{h,j} \rangle)^2 \right) \right\} \\
&\quad \times \frac{\left\{ \sum_{h=1}^p W(h) \left( \sum_{i,j=1}^{d_h} \langle (\kappa_0^{(h)} - \kappa_1^{(h)}) \nu_{h,i}, \nu_{h,j} \rangle^2 \right)^{1/2} \right\}^2}{\left\{ \sum_{h=1}^p W(h) \left( \sum_{i,j=1}^{d_h} \langle (\kappa_0^{(h)} - \kappa_1^{(h)}) \nu_{h,i}, \nu_{h,j} \rangle^2 \right) \right\}^2} \\
&\leq 4pE \left\{ \max_h \left( \sum_{i,j=1}^{d_h} (y_{ij}^h - \langle \kappa_0^{(h)}(\nu_{h,i}), \nu_{h,j} \rangle)^2 \right) \right\} \\
&\quad \times \frac{(\tau_2^2 \vee 1)}{(\tau_1 \wedge 1)} \frac{1}{\sum_{h=1}^p \sum_{i,j=1}^{d_h} \langle (\kappa_0^{(h)} - \kappa_1^{(h)}) \nu_{h,i}, \nu_{h,j} \rangle^2}
\end{aligned}$$

□

The proof of Theorem 4 can be easily obtained from the following lemma. This is a similar result to Theorem 3.1 in Hörmann et al. (2010). We first briefly introduce the definition of  $L^p - m$ -approximable sequence.

**Definition 1.** A sequence  $(X_k : k \in \mathbb{N}) \in L^p(H)$  is called  $L^p - m$ -approximable if each  $X_k$  admits the representation

$$X_k = f(\epsilon_k, \epsilon_{k-1}, \dots),$$

where the  $\epsilon_k$  are i.i.d. elements taking values in a measurable space  $S$ , and  $f$  is a measurable function  $f : S^\infty \rightarrow H$ . More we assume that if  $(\epsilon'_k : k \in \mathbb{N})$  is an independent copy of  $(\epsilon_k : k \in \mathbb{N})$  defined on the same probability space, then letting

$$X_k^{(m)} = f(\epsilon_k, \epsilon_{k-1}, \dots, \epsilon_{k-m+1}, \epsilon'_{k-m}, \epsilon'_{k-m-1}, \dots),$$

we have

$$\sum_{m=1}^{\infty} (E \|X_m - X_m^{(m)}\|^p)^{1/p} < \infty.$$

**Lemma 1.** Suppose  $(X_k: k = 1, \dots, N)$  is an  $L^4$ -m-approximation sequence with second moment  $c_h(t, s) = E(X_k(t)X_{k+h}(s))$ . Then for each lag  $h$ , there is some constant  $U_h < \infty$ , which does not depend on  $N$ , such that

$$NE\|\hat{c}_h - c_h\|_{\mathcal{S}}^2 \leq U_h,$$

where  $U_h$  is

$$\nu_4^4(X) + 4\sqrt{2}E\|X\|_4^3 \sum_{r=1}^{\infty} E\|X_1 - X_1^{(r+h)}\|_4$$

The proof of Lemma 1 is similar to that of Theorem 3.1 in Hörmann et al. (2010). We briefly show the basic steps as follows.

*Proof.* We can show  $\hat{c}_h$  is Hilbert-Schmidt operator. Then we have

$$NE\|\hat{c}_h - c_h\|_{\mathcal{S}}^2 = N \int \int \text{Var} \left[ \frac{1}{N} \sum_{k=1}^{N-h} (X_k(t)X_{k+h}(s) - E[X_k(t)X_{k+h}(s)]) \right] dt ds,$$

Set  $Y_n = X_k(t)X_{k+h}(s) - E[X_k(t)X_{k+h}(s)]$ , since  $X_k(t)$  is stationary, then

$$\text{Var} \left( \frac{1}{N} \sum_{k=1}^{N-h} Y_k \right) = \frac{1}{N} \sum_{|r| < N-h} \left( 1 - \frac{h+|r|}{N} \right) \text{Cov}(Y_1, Y_{1+r}),$$

and so

$$N \text{Var} \left( \frac{1}{N} \sum_{k=1}^{N-h} Y_k \right) \leq \text{Var}(Y_1) + 2 \sum_{r=1}^{\infty} |\text{Cov}(Y_1, Y_{1+r})|,$$

Setting  $Y_n^{(m)} = X_k^{(m)}(t)X_{k+h}^{(m)}(s) - E[X_k^{(m)}(t)X_{k+h}^{(m)}(s)]$ , we have

$$|\text{Cov}(Y_1, Y_{1+r})| = |\text{Cov}(Y_1, Y_{1+r} - Y_{1+r}^{(r+h)})| \leq [\text{Var}(Y_1)]^{1/2} [\text{Var}(Y_{1+r} - Y_{1+r}^{(r+h)})]^{1/2}$$

Therefore we have  $\int \int |\text{Cov}(Y_1, Y_{1+r})| dt ds$  is bounded by

$$\int \int [\text{Var}(X_1(t)X_{1+h}(s))]^{1/2} [\text{Var}(X_{1+r}(t)X_{1+r+h}(s) - X_{1+r}^{(r+h)}(t)X_{1+r+h}^{(r+h)}(s))]^{1/2} dt ds \quad (A1)$$

By the inequality  $|ab - cd|^2 \leq 2a^2(b - d)^2 + 2d^2(a - c)^2$

$$\begin{aligned} (A1) &\leq \sqrt{2} \int \int [E(X_1^2(t)X_{1+h}^2(s))]^{1/2} [EX_{1+r}^2(t)(X_{1+r+h}(s) - X_{1+r+h}^{(r+h)}(s))^2]^{1/2} dt ds \\ &\quad + \sqrt{2} \int \int [E(X_1^2(t)X_{1+h}^2(s))]^{1/2} [E(X_{1+r+h}^{(r+h)}(s))^2(X_{1+r}(t) - X_{1+r}^{(r+h)}(t))^2]^{1/2} dt ds \end{aligned} \quad (A2)$$

$$(A3)$$

For the first summand, by Cauchy-Schwarz inequality, we obtain

$$\begin{aligned} (A2) &\leq \sqrt{2} E\|X\|_4^2 \left( E \left[ \int X_{1+r}^2(t) dt \int \left( X_{1+r+h}(s) - X_{1+r+h}^{(r+h)}(s) \right)^2 ds \right] \right)^{1/2} \\ &= \sqrt{2} E\|X\|_4^3 E\|X_1 - X_1^{(r+h)}\|_4 \end{aligned}$$

Similar argument can be applied to the second summand to get the same upper bound, and we have

$$(A3) \leq \sqrt{2} E\|X\|_4^3 E\|X_1 - X_1^{(r+h)}\|_4$$

And obviously,  $\int \int \text{Var}(Y_1) dt ds \leq \nu_4^4(X)$ . Consequently,  $NE\|\hat{c}_h - c_h\|_{\mathcal{S}}^2$  is bounded by the  $U_h$ .  $\square$

*Proof of Theorem 4.* It is obvious that

$$\begin{aligned}
& E \left\{ \|(\hat{\kappa}_0^{(h)} - \hat{\kappa}_1^{(h)})^2 - (\kappa_0^{(h)} - \kappa_1^{(h)})^2\|_{\mathcal{S}}^2 \right\} \\
& \leq E \left\{ \|(\hat{\kappa}_0^{(h)})^2 - (\kappa_0^{(h)})^2\|_{\mathcal{S}}^2 \right\} + E \left\{ \|(\hat{\kappa}_1^{(h)})^2 - (\kappa_1^{(h)})^2\|_{\mathcal{S}}^2 \right\} \\
& + E \left\{ \|\hat{\kappa}_0^{(h)}(\hat{\kappa}_1^{(h)}) - \kappa_0^{(h)}(\kappa_1^{(h)})\|_{\mathcal{S}}^2 \right\} + E \left\{ \|\hat{\kappa}_1^{(h)}(\hat{\kappa}_0^{(h)}) - \kappa_1^{(h)}(\kappa_0^{(h)})\|_{\mathcal{S}}^2 \right\}
\end{aligned}$$

We only consider the first summand, and the same argument can be applied to the other summands. We have

$$\begin{aligned}
E \left\{ \|(\hat{\kappa}_0^{(h)})^2 - (\kappa_0^{(h)})^2\|_{\mathcal{S}}^2 \right\} & \leq E \left\{ \|\kappa_0^{(h)}(\hat{\kappa}_0^{(h)} - \kappa_0^{(h)})\|_{\mathcal{S}}^2 \right\} \\
& + E \left\{ \|(\hat{\kappa}_0^{(h)} - \kappa_0^{(h)})(\kappa_0^{(h)})\|_{\mathcal{S}}^2 \right\} \\
& + E \left\{ \|(\hat{\kappa}_0^{(h)} - \kappa_0^{(h)})^2\|_{\mathcal{S}}^2 \right\},
\end{aligned}$$

and by inequality  $\|AB\|_{\mathcal{S}} \leq \|A\|_{\mathcal{S}}\|B\|_{\mathcal{S}}$  and Lemma 1, it converges to zero.  $\square$

## B Computational fPCA of multivariate functional data

### B.1 Computation of eigenfunctions of $C_i(x)$

Ramsay (2004) described two computation methods of eigenfunctions. The first method is discretizing the functions. Suppose we have  $M$  sets of functions  $(x_{km}(t): m = 1, \dots, M, k = 1, \dots, N)$ , while the functions in each sets are discretized to a grid of  $l$  equally spaced values  $x_{km}(t_j)$ ,  $j = 1, \dots, l$ . Then the eigenvector of the covariance matrix of the concatenated discretized function  $((\mathbf{x}_{k1}^T, \dots, \mathbf{x}_{kM}^T)': k \in \mathbb{N})$  is very close to the eigenfunction of the covariance operator of the concatenated functions, where

$\mathbf{x}_{km} = (x_{km}(t_1), \dots, x_{km}(t_l))'$ . In practice, the number of grids may be much larger than the sample size  $N$ . The dimension of the covariance matrix of the concatenated discretized function is  $Ml \times Ml$ , which can be huge.

Another way, which is a bit more complicated but more efficient, is to represent the functions by a common set of basis. Suppose each function has the basis expansion

$$x_{km}(t) = \sum_{j=1}^J c_{km,j} \phi_j(t). \quad (\text{B-1})$$

and  $J$  is selected such that the above expansion is a reasonable approximation of the original functions. Let  $\tilde{x}_m = (x_{1m}, \dots, x_{Nm})'$ ,  $\tilde{x} = (\tilde{x}_1, \dots, \tilde{x}_M)$ ,  $\tilde{C}_m = \{c_{km,j}\}_{k,j=1}^{N,J}$ ,  $\tilde{\mathbf{C}} = (\tilde{C}_1, \dots, \tilde{C}_M)$ , and  $\tilde{\phi} = \mathbf{I}_M \otimes (\phi_1, \dots, \phi_J)'$ , where  $\mathbf{I}_M$  is a  $M \times M$  identity matrix. Then (B-1) can be expressed as a more compact form

$$\tilde{x} = \tilde{\mathbf{C}} \tilde{\phi}.$$

Then the estimated second moment is

$$\hat{c}(t, s) = \frac{1}{N} \tilde{\phi}(t)' \tilde{\mathbf{C}}' \tilde{\mathbf{C}} \tilde{\phi}(s).$$

Now suppose that an eigenfunction of  $\hat{c}(t, s)$  has the following basis expansion

$$\hat{\nu}(t) = \left( \sum_{j=1}^J b_{1j} \phi_j(t), \dots, \sum_{j=1}^J b_{Mj} \phi_j(t) \right)' = \tilde{\phi}(t)' \tilde{\mathbf{b}},$$

where  $\tilde{\mathbf{b}} = (\mathbf{b}_1, \dots, \mathbf{b}_M)'$ , where  $\mathbf{b}_m = (b_{m1}, \dots, b_{mJ})$ , this yields

$$\begin{aligned} \int \hat{c}(t, s) \hat{\nu}(s) ds &= \int \frac{1}{N} \tilde{\phi}(t)' \tilde{\mathbf{C}}' \tilde{\mathbf{C}} \tilde{\phi}(s) \tilde{\phi}(s)' \tilde{\mathbf{b}} ds \\ &= N^{-1} \tilde{\phi}(t)' \tilde{\mathbf{C}}' \tilde{\mathbf{C}} \tilde{W} \tilde{\mathbf{b}} \\ &= \lambda \tilde{\phi}(t)' \tilde{\mathbf{b}}, \end{aligned}$$



where  $\tilde{W} = \mathbf{I}_M \otimes W$ , and  $W_{ij} = \int \phi_i \phi_j$ . This equation holds for arbitrary  $t$ , thus we have

$$N^{-1} \tilde{W}^{1/2} \tilde{\mathbf{C}}' \tilde{\mathbf{C}} \tilde{W}^{1/2} \mathbf{u} = \lambda \mathbf{u},$$

where  $\mathbf{u} = \tilde{W}^{1/2} \tilde{\mathbf{b}}$ . We solve the eigenvector of  $\tilde{W}^{1/2} \tilde{\mathbf{C}}' \tilde{\mathbf{C}} \tilde{W}^{1/2}$ , and the eigenfunction of  $\hat{c}(t, s)$  will be  $\tilde{\phi}(t)' \hat{\mathbf{b}}$ . Note that the dimension of  $\tilde{W}^{1/2} \tilde{\mathbf{C}}' \tilde{\mathbf{C}} \tilde{W}^{1/2}$  is  $MJ \times MJ$ , and  $J$  is typically much smaller than  $l$ .

## B.2 Computation of eigenfunctions of $C = (C_0 - C_1)^2$

The estimator of  $C$  can be approximated by

$$\begin{aligned} (\hat{c}_0 - \hat{c}_1)^2 &= \left( \frac{1}{n_0} \tilde{\phi}(t)' \tilde{\mathbf{C}}'_0 \tilde{\mathbf{C}}_0 \tilde{\phi}(s) - \frac{1}{n_1} \tilde{\phi}(t)' \tilde{\mathbf{C}}'_1 \tilde{\mathbf{C}}_1 \tilde{\phi}(s) \right)^2 \\ &= \int \tilde{\phi}(t)' \left( \frac{1}{n_0} \tilde{\mathbf{C}}'_0 \tilde{\mathbf{C}}_0 - \frac{1}{n_1} \tilde{\mathbf{C}}'_1 \tilde{\mathbf{C}}_1 \right) \tilde{\phi}(t_0) \tilde{\phi}(t_0)' \left( \frac{1}{n_0} \tilde{\mathbf{C}}'_0 \tilde{\mathbf{C}}_0 - \frac{1}{n_1} \tilde{\mathbf{C}}'_1 \tilde{\mathbf{C}}_1 \right) \tilde{\phi}(s) dt_0 \\ &= \tilde{\phi}(t)' \left( \frac{1}{n_0} \tilde{\mathbf{C}}'_0 \tilde{\mathbf{C}}_0 - \frac{1}{n_1} \tilde{\mathbf{C}}'_1 \tilde{\mathbf{C}}_1 \right) \tilde{W} \left( \frac{1}{n_0} \tilde{\mathbf{C}}'_0 \tilde{\mathbf{C}}_0 - \frac{1}{n_1} \tilde{\mathbf{C}}'_1 \tilde{\mathbf{C}}_1 \right) \tilde{\phi}(s). \end{aligned}$$

By the same argument, we have

$$\tilde{W}^{1/2} \left( \frac{1}{n_0} \tilde{\mathbf{C}}'_0 \tilde{\mathbf{C}}_0 - \frac{1}{n_1} \tilde{\mathbf{C}}'_1 \tilde{\mathbf{C}}_1 \right) \tilde{W} \left( \frac{1}{n_0} \tilde{\mathbf{C}}'_0 \tilde{\mathbf{C}}_0 - \frac{1}{n_1} \tilde{\mathbf{C}}'_1 \tilde{\mathbf{C}}_1 \right) \tilde{W}^{1/2} \mathbf{u} = \lambda \mathbf{u},$$

where  $\mathbf{u}$  is the eigenvector of the above eigen-equation. Then the eigenfunction of  $C$  is  $\tilde{\phi}(t)' \tilde{W}^{-1/2} \mathbf{u}$ .

## C Additional figures

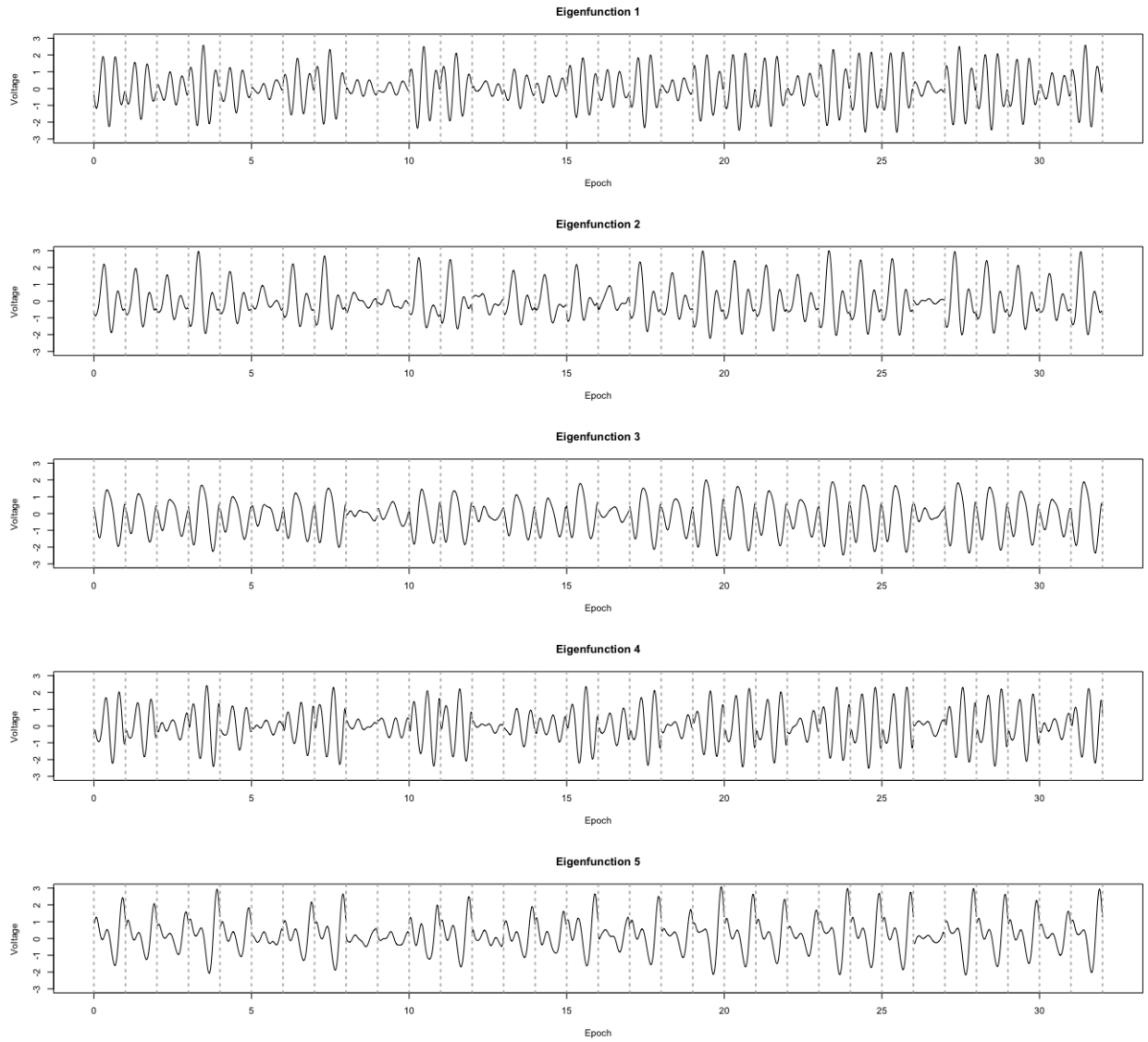


Figure 11: The first 5 principal components of  $(\hat{\mathcal{C}}_0 - \hat{\mathcal{C}}_1)^2$ . Each functional principal component has 32 segments, corresponding to 32 channels.

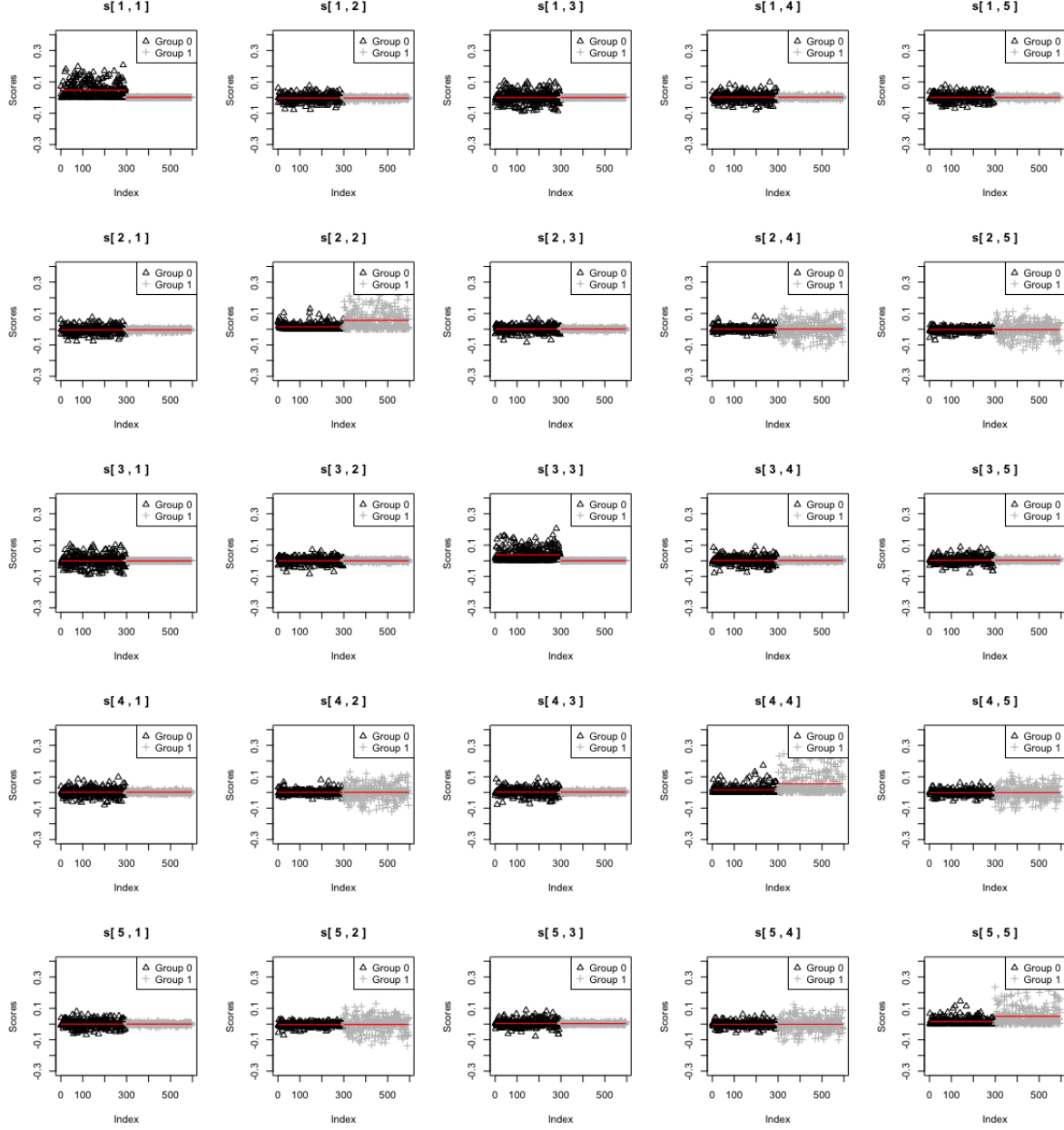


Figure 12: Scores of the first 5 principal components of  $(\hat{C}_0 - \hat{C}_1)^2$